Geomorphology 408 (2022) 108237

Contents lists available at ScienceDirect

Geomorphology

journal homepage: www.journals.elsevier.com/geomorphology

The modern wave-induced coastal staircase morphology along the western shores of the Dead Sea

Yehouda Enzel[a,*], Amit Mushkin[b], Matias Groisman[a,b], Ran Calvo[b], Haggai Eyal[a,b], Nadav Lensky[a,b]

[a] The Fredy & Nadine Herrmann Institute of Earth Sciences, The Hebrew University, Edmond J. Safra Campus, Givat Ram, Jerusalem 9190401, Israel
[b] Geological Survey of Israel, 32 Yesha'ayahu Leibowitz St., Jerusalem 9692100, Israel

ARTICLE INFO

Keywords:
Coastal cliffs
Dead Sea
Waves
Wind storms

ABSTRACT

This research provides insights into the formation of the coastal cliffs comprising the staircase morphology along the western coast of the Dead Sea as a result of its anthropogenic, regressive modern (last ~50 years) lake-level fall. The analysis of this morphology is based on observations and measurements of the impact of seasonal lake-level rises of 0–0.2 m and 0.7–2 m in normal versus exceptionally wet winters, respectively. We conducted repeated detailed topographic surveys of the shores for characterizing the evolving morphology with time, and coupled them with wind speed and wave amplitude during cliff formations. The detailed lake-level curve and the almost monotonic level decline allow associating each cliff with the exact year and season of its formation. This detailed chronology allowed, in turn, to identify and associate the pronounced and well-documented seasonality in the lake-level fall with the wind and wave data during specific seasons, years, and multi-year episodes. As a result, we can point at the controlling processes and environmental conditions for cliff formation. Under the regional Mediterranean climate with its distinct seasonality, winters are characterized by eastern Mediterranean low-pressure systems, generating the Jordan River flow in its northern headwaters and its discharge into the lake; this discharge controls the level fluctuations. At the Dead Sea area, these winter systems precipitate little. However, they generate high winds and storm waves that erode an additional coastal cliff at the base of the preexisting staircase every winter. Therefore, at the seasonal scale, a clear separation exists between (a) individual, cliff-forming, stronger wind storms operating only during winters under relatively stable water levels, and (b) the ~1-m annual lake-level fall, mostly during summers. This pronounced seasonality in both the wind and lake level (a) dictates the seasonal pace of cliff formation at vertical intervals similar to the magnitude (~1 m) of the annual lake-level fall by evaporation and artificial brine diversion, and (b) facilitates the cliff separation in the landscape. This regular pacing by winter storms, the minor lake-level rises, and the annual evaporation and diversion support the preservation of the individual cliffs that assemble into the staircase morphology in the coarse-clastic delta fronts and mudflats characterizing the recently emerging coast. Anomalous lake-level rises during exceptionally wet winters are more erosive, even with regular wind storms; they create the largest lateral erosion. Under the emerging shore topography, which results from the steep bathymetry, the outcome is cliffs often much higher than the respective amplitude of their causative lake-level rises. This depends on the duration of the rise and of individual storms and indicates that under the variance of the modern hydroclimatology, the abnormal seasonal lake-level rises operating with regular winter storms, can aggressively erode the shore.

Proposed plans to stabilize or raise the falling water level of the Dead Sea would induce coastal erosion and stream incision, which would threaten the existing highway and other infrastructure built close to its shore.

1. Introduction

Coastal cliffs are widespread landforms around the world's shores (Emery and Kuhn, 1982). These landforms are studied for understanding their formation, maintenance, and evolution, and, in part, because of their storm- to decadal-scale erosional retreats, which affect coastal communities, infrastructure, and historical sites (e.g., Sunamura, 1988; Bray and Hooke, 1997; Stewart and Vita-Finzi, 1998; Dickson et al.,

* Corresponding author.
E-mail address: yehouda.enzel@mail.huji.ac.il (Y. Enzel).

https://doi.org/10.1016/j.geomorph.2022.108237
Received 30 May 2021; Received in revised form 27 March 2022; Accepted 30 March 2022
Available online 2 April 2022
0169-555X/

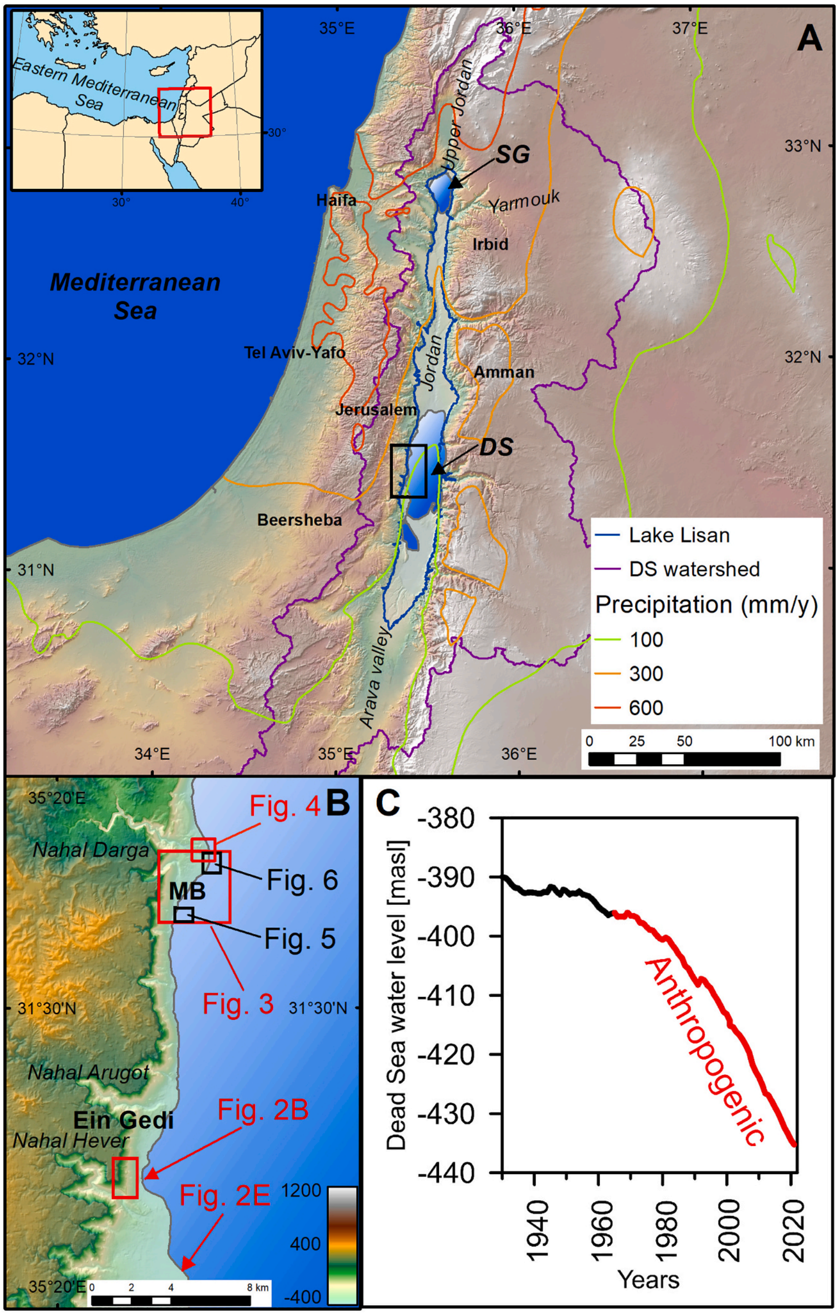

Fig. 1. (A) Location map of the Dead Sea (DS), its watershed, and the extent of its predecessor, The Late Pleistocene Lake Lisan during its highest stand (blue line), covered the area from the northern Arava valley and the Sea of Galilee (SG). Note that the main discharge to the Dead Sea arrives from the wetter watersheds of the Yarmouk and upper Jordan Rivers through the lower Jordan River (B) locations of specific study sites at the delta of Nahal Darga and at Mineral Beach (MB) located along the western shores of the deep northern basin of the Dead Sea. (C) Annually measured modern Dead Sea level curve (masl = meters above sea level) (Israel Hydrological Service, 2015). The current Dead Sea level is at 437 m below sea level. Note that the diversion of water begun in 1964 (and level since is marked in red) with a large diversions from the Sea of Galilee and the Yarmouk River caused the lake level to drop faster since ca. 1970. (For interpretation of the references to color in this figure legend, the reader is referred to the web version of this article.)

2007; Naylor et al., 2010; Wong et al., 2014; Young and Carilli, 2019; Mushkin et al., 2019; Young et al., 2021). Coastal cliff erosion is a global challenge enhanced by global warming, its associated sea-level rise, and frequency changes in extreme wind and storm waves. This growing concern for coastal environments (e.g., Hackney et al., 2013) and estimating coastal erosion under sea-level changes (e.g., Walkden and Hall, 2005; Dawson et al., 2009; Nicholls and Cazenave, 2010; Mushkin et al., 2016) can benefit from a better understanding of the controlling wind and waves generated by the extreme storms (Young et al., 2021). Efforts toward this goal are based on detailed modern surveys and historical data (Katz and Mushkin, 2013; Young et al., 2021), predictive empirical or process-based computerized modeling (see early summary by Bray and Hooke, 1997; Walkden and Hall, 2005), up-scaling from laboratory physical experiments, or observations of coastal cliff associated with the 10–150-m eustatic, glacial-interglacial scale (i.e., 10^3–10^6 years) of sea-level changes, sometimes associated with large-scale tectonics (Stewart and Vita-Finzi, 1998; Mackey et al., 2014; Huppert et al., 2020; Malatesta et al., 2021). Most available measurements are based on modern coastal cliffs and their respective shore platform, generated under minor sea-level changes and/or tides (Bray and Hooke, 1997; Hall et al., 2002; Walkden and Hall, 2005; Dickson et al., 2007; Collins and Sitar, 2008; Le Cossec et al., 2011; Katz and Mushkin, 2013; Barnard et al., 2014; Hurst et al., 2016; Vitousek et al., 2017). Such observations drive coastal-erosion predictions but are still limited by the resolution of vertical and lateral erosion.

Coasts surrounding inland terminal and especially around amplifying lakes (sensu Street-Perrott and Harrison, 1985) can provide additional insights. They are formed, maintained, and change under relatively large amplitudes (1 to >100 m) of seasonal to millennial water-level changes, and preserve evidence for coastal erosion throughout their history (Bowman, 1971; Abu Ghazleh and Kempe, 2009; Abu Ghazleh et al., 2011; Oviatt et al., 2015; Jewell, 2016;

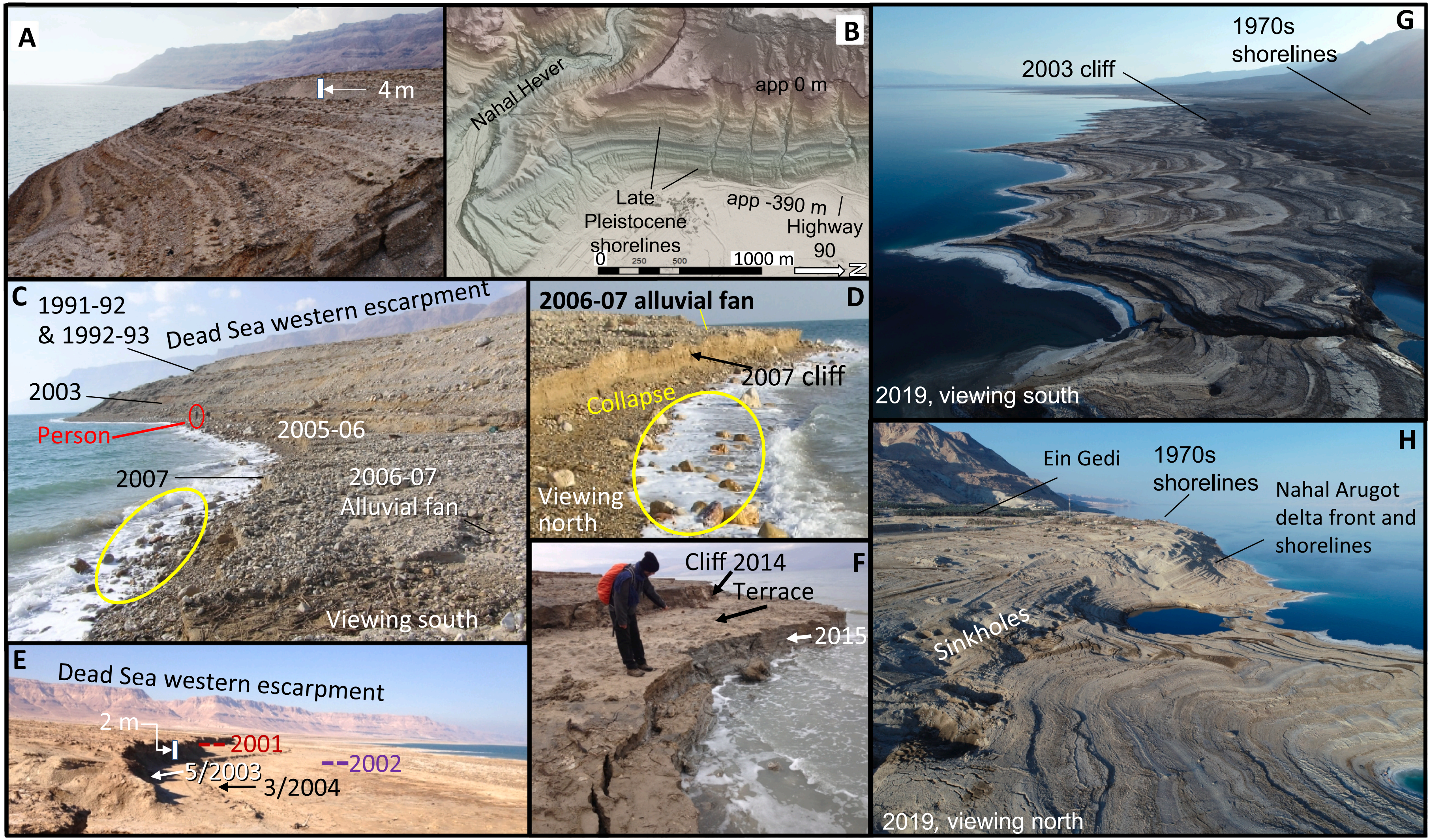

Fig. 2. (A) Cliff staircase morphology (in 2019) of the Nahal (Wadi) Darga delta front (location of Nahal Darga is in Fig. 1B within the area marked as Fig. 6; view is to the south) developed since the exposure of the delta front in the early 1970s. The smallest scarps are ~1 m high (photograph by Liran Ben Moshe, Geological Survey of Israel). (B) DEM showing the latest Pleistocene shorelines and coastal cliffs developed on the coarse clastic delta front of Nahal Hever and the escarpment of the Dead Sea rift during the falling of Lake Lisan from its last glacial maximum high stand. (C) and (D): Photographs of the steep delta front of the Nahal Darga and its shorelines and wave-cut cliffs in late winter of 2007. Note that Fig. 2A shows the same delta front in 2019 and the large, 4-m-high 1991–1992 cliff that formed following the relatively large (>2 m) lake level rise of wet and stormy winter (see text). The ~2.5-m high 2003 cliff was produced by a 0.7-m lake-level rise. The other cliffs were formed by minor winter storm waves and minor winter season level rises (e.g., the 2007 cliff). Yellow ellipsoids marks the same gravel in 2C and 2D. (E) Wave-cut cliffs in the mudflat of Nahal Zeelim (See 5E in Fig. 1). The ~3.5-m-high cliff (maximum height) was formed during an erosional transgressive lake-level rise in 2003. This cliff stands out along the western shores of the Dead Sea. Horizontal lines mark the location and height of respective shores taken from the lake-level curve and from topographic surveys. The dashed lines mark the 2001 and 2002 shorelines (in the air) before their erosion by the 2003 rising lake. (F) A minor, regular winter cliff in the relatively steep eastern edge of a mudflat was observed during its final formation in the winter of 2015. Note the abandoned 2014 cliff and terrace. (G) and (H) are general views of the coast taken from south of the delta front of Nahal Arugot (Fig. 1B) to south and north at the vicinity of Ein Gedi (Both by Liran Ben Moshe, Geological Survey of Israel). (For interpretation of the references to color in this figure legend, the reader is referred to the web version of this article.)

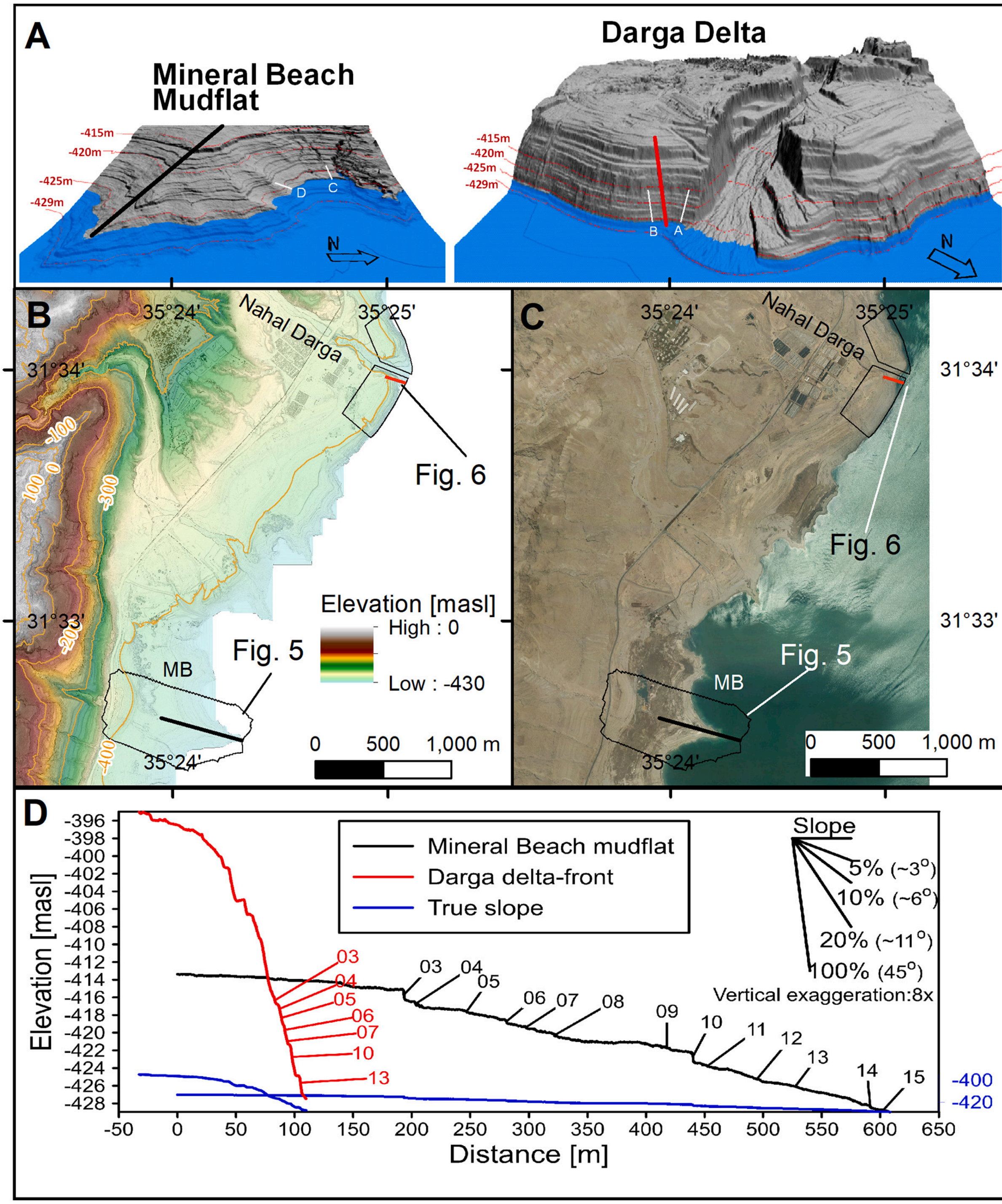

Fig. 3. (A) and (B): Topography and aerial photograph of the Nahal Darga and Mineral Beach sites (locations in Fig. 1B). (C) Two selected topographic profiles (with locations in (A) and (B)), presented without (in blue) and with 8× vertical exaggeration (in red and black lines). Note the steep delta front of Nahal Darga (in red) with the 1992 cliff and the pronounced 2003 and 2010 cliffs in the mudflat (in black). masl = meters above sea level. (For interpretation of the references to color in this figure legend, the reader is referred to the web version of this article.)

Schuster and Nutz, 2018; Roland et al., 2021). Because of, yet, limited observations, their widespread availability remains an untapped resource for enriching the insights into controlling processes and changes during diverse rising and falling lake-level trends. Here, we turn to the Dead Sea (Fig. 1A, B), an observation-rich fluctuating terminal lake, with several advantages for such research (see Section 2, below). Enzel et al. (2006), Enzel and Bar-Yosef (2017), and Stein and Goldstein (2020) presented information-rich updated background on the Dead Sea, its levels and chronology, including of its predecessor Late Pleistocene Lake Lisan (Fig. 1A); these summaries also include current and past regional climates and the characteristic sedimentology.

Our goal here is to understand and quantify the governing drivers of coastal erosion along the Dead Sea shores and respective cliff formations. Specifically, such lake-based research can provide diverse analogs documenting the (a) responses of shores to hydrological budget reflected in positive and negative water-level (Fig. 1C) changes, and (b) climatic forcing of wind and waves that generate these cliffs at a sub-seasonal to multi-year temporal scales. Our research questions include: (a) At which

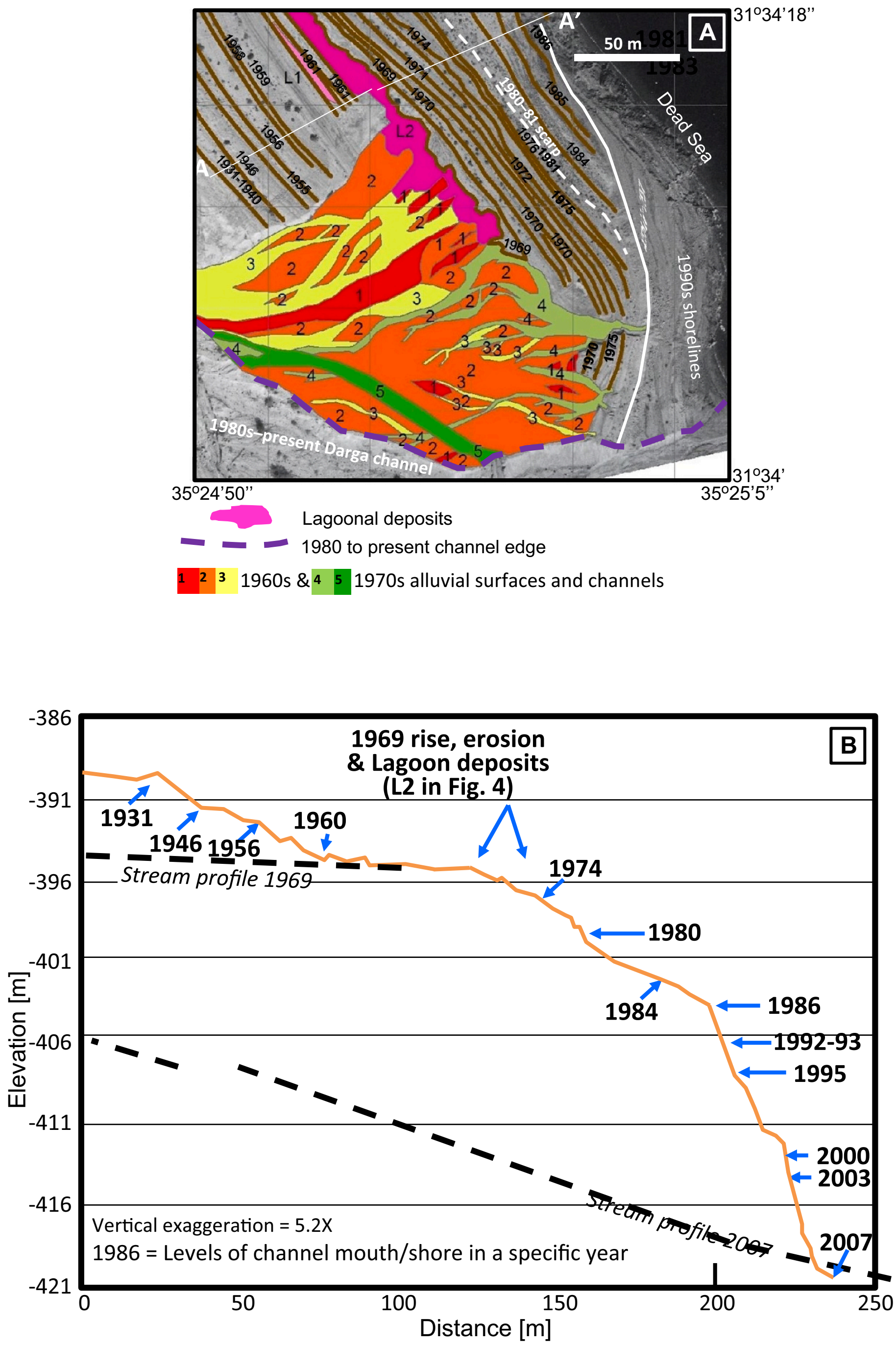

Fig. 4. (A) Laterally-shifting alluvial fan segments (1–3) of Nahal Darga north of the 1980s to present edge of the incised channel. Surface 4 is related to the initial exposure of the delta front (and a few subsequent years) and Surface 5 is the last channel before the 1980s channel incision. Also mapped are the recessional shorelines developed on the steep delta front since the early 1970s. Specifically marked are the two largest cliffs, which were formed during the wet winter seasons of 1979–1980 and 1991–1992, respectively. Note the convergence of these two shorelines. (B) The A-A′ topographic cross-section (marked in Fig. 4A) in brown was measured with EDM and presents selected Dead Sea levels (and recognized shores and cliffs). Note (i) the association of these segments with the coeval late 1960s to earliest 1970s mapped shorelines, (ii) fine-grained lagoon deposits L1 and L2 (1961 and 1969, respectively), were deposited when a transgressive shoreline blocked the flow on the alluvial fan. (For interpretation of the references to color in this figure legend, the reader is referred to the web version of this article.)

temporal scale do cliffs form, erode, and retreat landward, and, as a result, amplify their heights? (b) What are the impacts of rising and falling lake levels on cliff formation? We stress that in the case of the Dead Sea these water levels' rise and falls are associated, respectively, with transgressions and regressions. (c) What is the role of individual large storms? (d) What is the role of the regional hydroclimatology that generates cliff formation?

We first introduce the Dead Sea and its coastal environments (Section 2). Section 3 summarizes our approach and the methodologies applied. Then, in Section 4, we examine and quantify impacts of individual storms, demonstrating the sub-seasonal to annual pattern of coastal erosion under the regressive Dead Sea level lowering in the last five decades to complement these storm-scale erosions. In Section 5, we documented impacts of relatively rare, modern, transgressive sub-seasonal to annual lake-level rises under wet winters. These rises are exceptions to the decades-long, lake-level lowering, regressive phase and teach us the potential of transgressive erosion. Later, in Section 6, we view the staircase morphology of the last decades as a whole. In Section 7, we discuss how regional hydroclimatology, level changes, windstorms, and waves drive modern coastal erosion in the Dead Sea. Finally, in Section 8, we point to implications for processes operated at other friable or unconsolidated sediment coastal cliffs including preservation in the Quaternary geological record of major coastal features and sediments and to the debated Red-Dead Project.

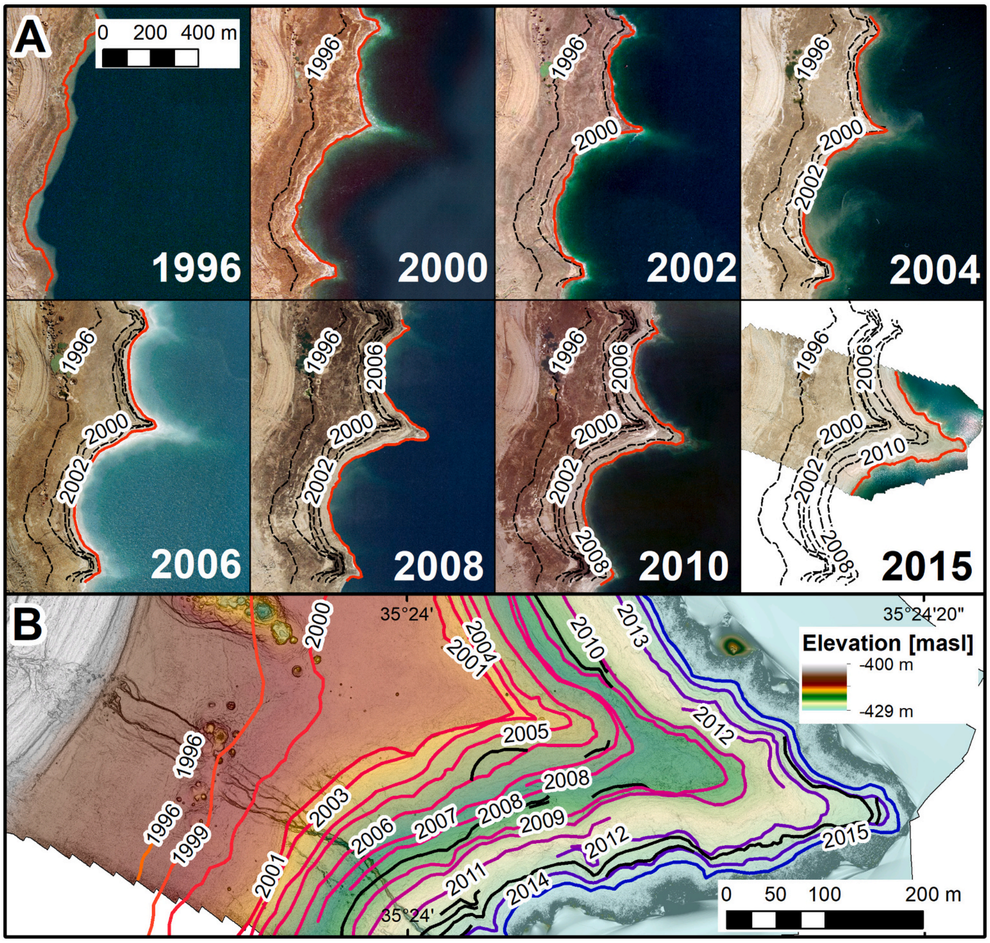

Fig. 5. Aerial expression of a series of coastal cliffs in Mineral Beach site. (A) The altitudes of selected (1996–2015) Dead Sea shorelines were mapped and digitized on the aerial ortho-photographs (see Section 3). (B) Coastal cliffs mapped on the LiDAR-based DEM. We combined the measured shorelines with the high-resolution lake-level data and the specific year is labeled based on the associated lake level-year (Fig. 1). Part of this map is expanded in Fig. S1.

2. Field setting: the coastal environments of the Dead Sea

The Dead Sea is currently a 280-m-deep hypersaline terminal lake with a current water density ≈1.24 g cm^{-3} (Arnon et al., 2016; Sirota et al., 2016) occupying the lowest area on the continental Earth (Enzel et al., 2006). Its current water level (2021) is at −437 masl (meters above sea level). The Dead Sea is characterized by fluctuating lake levels at much greater rates than the levels of oceans and seas. The changes in the vertical and lateral positions of the Dead Sea shores are larger than in laboratory experiments, and therefore, they can provide detailed, well-measured analogs and insights on the processes controlling the formation of the ubiquitous modern coastal cliffs (e.g., Fig. 2).

Along the western and eastern edges of the lake, there are distinct shorelines that formed during high stands, falling, and fluctuating phases of the Late Pleistocene Lake Lisan (Figs. 1A, 2), the much larger and higher-level (~160–350 m below sea level) predecessor of the Dead Sea (Bowman, 1971; Abu Ghazleh and Kempe, 2009; Bartov et al., 2002; Bartov et al., 2003; Torfstein et al., 2013; Torfstein and Enzel, 2017) and by the lower stands (~370–430 m below sea level) of the Holocene Dead Sea.

The modern, Holocene and Pleistocene fan-deltas of the Dead Sea are composed of unconsolidated coarse-clastic gravel, interfingering with fine-grained lacustrine and well-sorted gravelly beach deposits (Sneh, 1979; Manspeizer, 1985; Bowman, 1997; Enzel et al., 2000; Bartov et al., 2006; Bookman et al., 2006; Waldmann et al., 2017; Eyal et al., 2019). The sedimentary sequences of these deltas are exposed by the deep incision of tributary streams following the rapid lake-level falls (Bartov et al., 2007, 2012; Bowman, 1971; Bowman et al., 2000; Enzel et al., 2000; Ben Moshe et al., 2008; Storz-Peretz et al., 2011), allowing a connection of modern observations with historical and earlier sedimentary sequences at the same site.

The relatively flat-top mudflats, sloping <0.5% toward the lake, are composed of unconsolidated but slightly cohesive laminated to well-bedded, silt-sized sediments (Fig. 2E). These subaqueous sediments have accumulated and trapped in the areas between the coarse-clastic deltas and along the retreating shore. Initial mudflat emergence above the water occurred in the early 1990s, following the fast-falling lake level (Figs. 2E and 3). At their eastern edges toward the receding lake, the slopes of the mudflat increase and provide field-scale analogs for the continental shelf edge and slope in the world oceans (Eyal et al., 2019; Dente et al., 2021).

These modern deltas and mudflats emerged asynchronously (Ben-Moshe, 2006) from underwater during the modern lake-level fall. Earlier, coarse-gravelly alluvial fans were in direct contact with the shore environment (together they practically comprise the topsets of the delta) and fed the now emerging underwater delta fronts (Fig. 4).

These shorelines and cliffs around the Dead Sea, raise the question regarding their formation, beyond the obvious observation that they mark higher lake stands. We focus here on the shores associated with this modern regressive lake with falling water level, mainly because of data availability and consider them as potential analogs and past occurrences. These modern shores are characterized by a staircase-like morphology with numerous, regularly near-one-meter-high cut cliffs (Figs. 2–4).

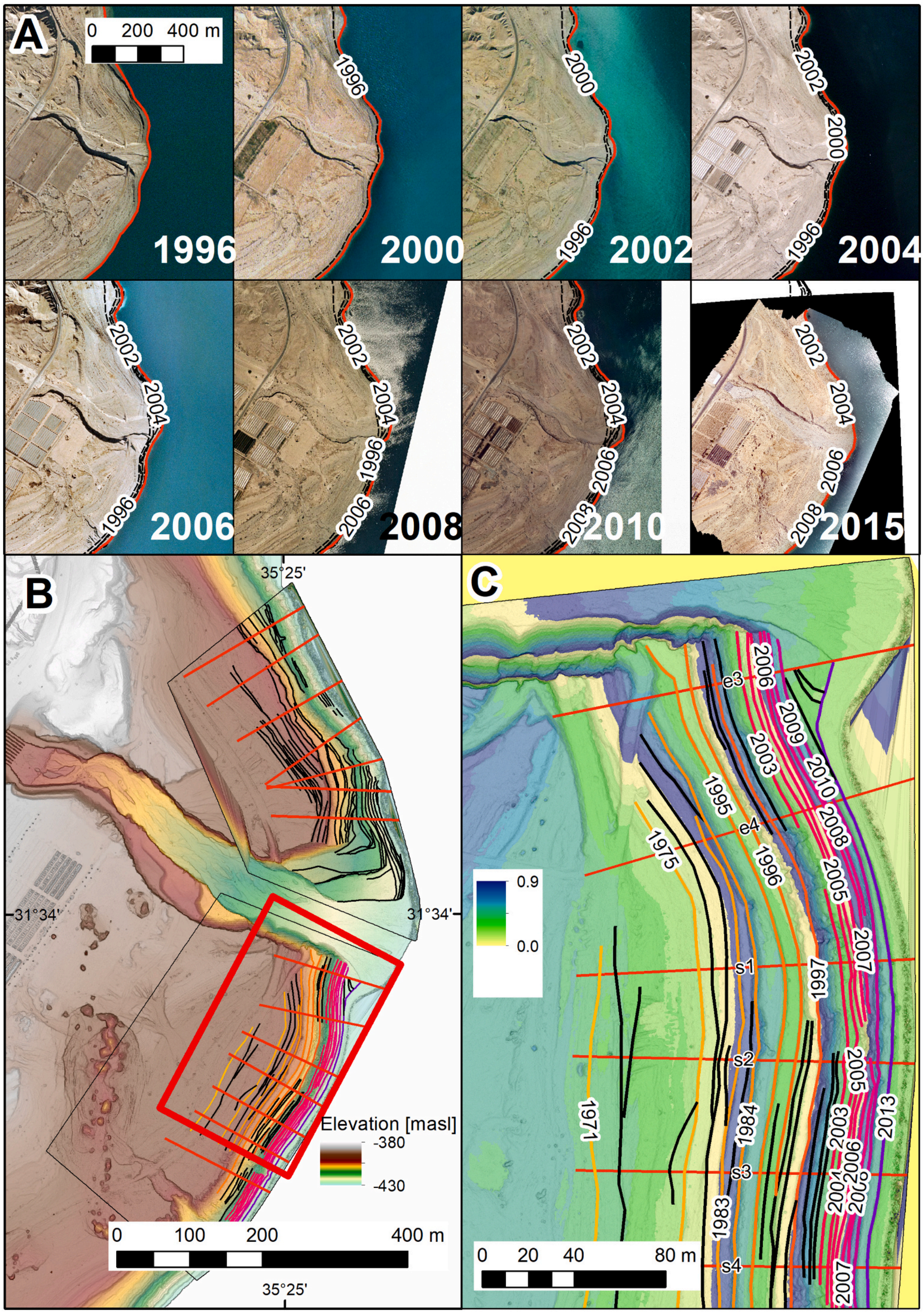

Fig. 6. Aerial expression of a series of coastal cliffs in the Nahal Darga delta site. (A) The altitudes of selected (1996–2015) Dead Sea shorelines were mapped and digitized on the aerial ortho-photographs (see Section 3). (B) Coastal cliffs mapped on the LiDAR-based DEM. (C) The expansion of the red box in (B). We combined the measured shorelines with the high-resolution lake-level data and then labeled the shoreline based on this lake level-year (Fig. 1).

We selected the western shores of the Dead Sea as our study sites because of the following reasons.

(a) Rapid, anthropogenic lake-level decline in the past decades (~1 m yr^{-1}; Lensky et al., 2005; Lensky and Dente, 2015; Fig. 1C) and the pronounced staircase shoreline morphology (Figs. 2–4).
(b) Diverse depositional environments into which the cliff staircases have been eroding, including the abovementioned, common unconsolidated coarse-gravelly delta fronts and soft-sediment silty mudflats.
(c) Distinct lake-level rises (Fig. 1C) occurring during the regionally wettest seasons, allowing the exploration of transgressive coastal cliffs.
(d) Distinct association between many individual cliffs and the well-studied synoptic and regional climatology including wind-wave forcing. This Mediterranean region presents a large difference between the wet winters and the totally dry summers (e.g., Kushnir et al., 2017). This seasonal contrast allows identifying coastal morphological changes during a full annual cycle.

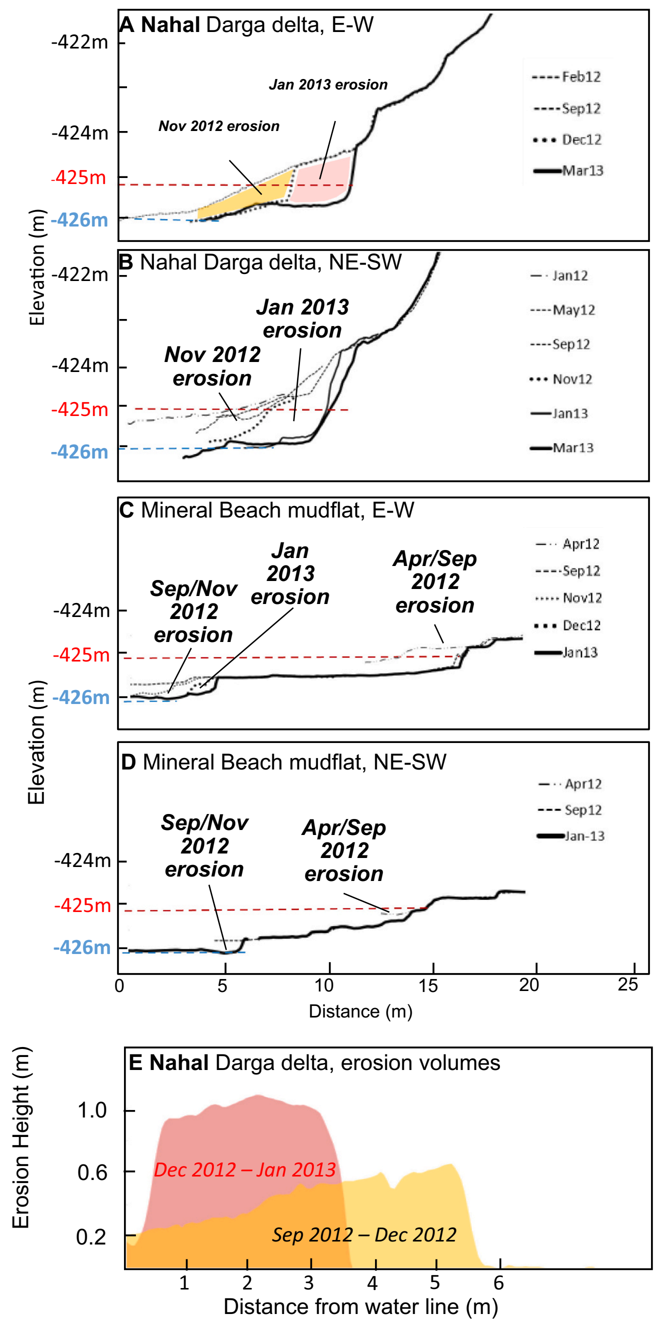

Fig. 7. Seasonal-scale dynamics. (A) and (B) Cliff-forming erosion events documented with 6–9 repeat ground-based LiDAR scans (cm-scale resolution) carried out between January 2012 and March 2013 at the Nahal Darga delta. Data for the two selected orientations are plotted at 5 cm resolution. (C) and (D) Cliff-forming erosion events documented with six repeat ground-based LiDAR scans (cm-scale resolution) carried out between April 2012 and January 2013 at the Mineral Beach mudflat. Data for the two selected orientations are plotted at 5 cm resolution. See Fig. 3A for location of cross-sections A–D. (E) Erosion as a function of distance from water line for the two primary cliff-forming intervals documented along the E-oriented Nahal Darga delta front profile in *A*. Orange: Sep 2012–Dec 2012 event; Red: Dec 2012–Jan 2013 event. (For interpretation of the references to color in this figure legend, the reader is referred to the web version of this article.)

(e) This hyperarid saline lake enables measuring the direct impacts of wind and waves on coastal cliffs changes; this is unlike wetter environments, where groundwater seepage and/or vegetation impact cliff formation and evolution in response to lake-level rises (e.g., Krueger et al., 2020)

From the quite long (>50 km) western shores of the northern Dead Sea, we focus on the two common coastal depositional environments (Fig. 1B) at (a) the Nahal (Wadi) Darga Holocene and modern steep, mostly coarse-gravel delta front with their continuous and curved shores (Figs. 2–4), and (b) The Mineral Beach mudflat with its pointing beachhead cape (Figs. 1 and 3), located 2 km south of that Nahal Darga delta.

3. Methods and data analyses

3.1. High-resolution topographic surveys using LiDAR and photogrammetry

To characterize coastal landform dynamics and processes associated with lake-level changes and individual storms, we focused on the two abovementioned selected sites. Since the late 1980s we used two-dimensional topographic profiles by a total station (Fig. 4). Later, in 2011 we conducted repeat terrestrial and airborne LiDAR (Light Detection and Ranging) scans as well as high-resolution photogrammetry (5-cm resolution, ‘structure for motion’, SfM) terrain modeling from a drone platform; most of the data presented is from the LiDAR and SfM. From these data (Fig. 7), we extracted the altitude, topography, and shapes of wave-cut scarps and their associated shorelines, stream terraces, alluvial fans, and delta fronts.

The terrestrial LiDAR scanner (TLS) (Leica ScanStation 2) was used to acquire ca. centimeter-resolution data in February, March, May, July, September, November, and December of 2012 and in January and March 2013 for an area of ~100 m^2 at the two selected sites. A Terrascan-B drone was used to acquire 5 cm/pixel DEMs of Mineral Beach mudflat in May 2015 and Nahal Darga delta in September 2015. Airborne LiDAR data (Fig. 7A), acquired at 4 pts/m^2 during April 2015 were used to examine the spatial variability of shore morphology across broader areas (each area is ~1000 m^2).

For ease of presentation, we only use a small portion of the DEM data as repeated 2D topographic profiles at the Nahal Darga delta front and the Mineral Beach mudflat. We present selected 2D profiles (Fig. 7) extracted from the time series of the 3D LiDAR data, to capture storm- to seasonal-scale morphologic changes during the February 2012–March 2013 interval.

We compared the different cross-sections constructed from the airborne LiDAR data (Fig. 7) with measurements from the Israel Hydrological Service, documenting monthly the lake levels at a ±2 cm accuracy since 1976. Together with the altitudes of individual shorelines measured in the field with GPS-RTK, the specific year and even season of individual shoreline formation could be determined. This was assisted by (a) at least, two annual field visits since 1991 to the sites with level measurements, and total station surveys once in a few years (tied with the respective lake level and/or benchmarks as a datum), and (b) ground and aerial photographs at improving resolutions over the last ~30 years (see Ben Moshe et al., 2008 for details).

3.2. Wind and waves

Wind and waves were measured during the 2012–2013 TLS campaigns. The wind was measured using a sonic anemometer (2-D WindSonic, Gill, UK), placed three meters above the shoreline. Wave activity was estimated using a pressure sensor (Submersible Pressure Transducer, CS 455, resolution: 0.175 mm; accuracy: 2 mm, Campbell, USA), following the procedure described by Nehorai et al. (2013). The average level across the Dead Sea has little lateral variability mainly because of the only <2-cm high daily seiche and tide amplitude below the resolution of the measured level (Arnon et al., 2014, 2019).

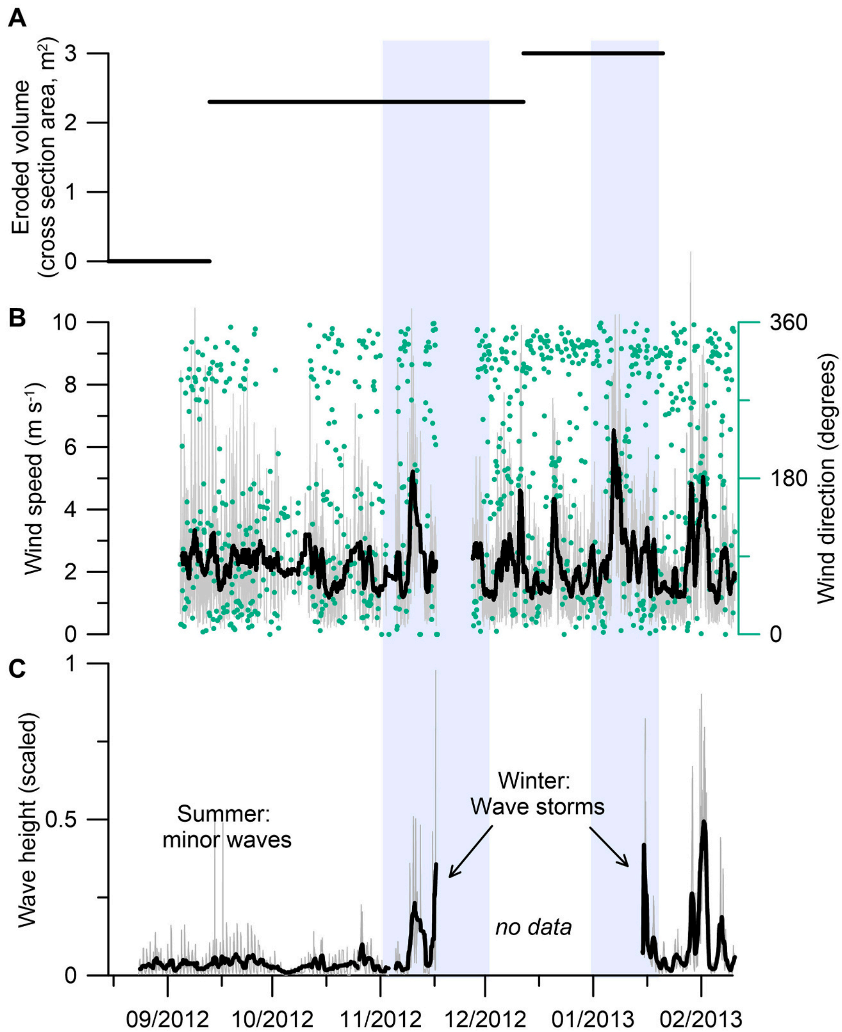

Fig. 8. Measured coastal erosion under hydrometeorological forcing, 2012–2013. (A) The eroded area in a cross section in m^2, which is also equivalent to volume of eroded material per 1 m of coastal length by the cliff retreat (see also Fig. 7). (B) Wind speed, 10-minute averages (grey) and one day moving average (black) recorded at Mineral Beach. Also presented is wind directions. (C) Wave amplitude as depicted by pressure transduces (i.e., scaled to maximum wave height, uncalibrated, see text). (D) The light blue background marks the respective meteorological thresholds estimated for generating erosion. The "no data" interval was caused by a cable torn by waves. (For interpretation of the references to color in this figure legend, the reader is referred to the web version of this article.)

4. Coastal cliff formation during falling, regressive lake levels

Most of the modern wave-cut cliffs along the Dead Sea shores are ~1-m high. This height fits the common vertical magnitude of the annual lake-level drop of 0.8–1.2 m yr^{-1} over the last three decades (Fig. 4). In this section we explore why the common step height is related to annual scale of level decline. As part of the effort to answer this, we conducted topographic surveys at an approximately monthly resolution to cover a full seasonal cycle of 2012–2013 (Groisman, 2013). We focus on potential drivers of the erosion: wind speed (not direction), storm waves, and the changes in lake level. The on-shore and bathymetry slopes are quite high. They are provided in specific figures below.

4.1. Winter: cliff formation during storms

The repeat TLS scans of the Nahal Darga delta front revealed that a 0.7-m-high coastal cliff formed between September and December 2012 (Fig. 7). Our field visits indicate that this cliff most probably formed during the storms that occurred in November 2012. The scans also indicated that during the one-month-long interval between December 2012 and January 2013 there was an additional 2.5–4 m of landward lateral cliff erosion with cliff height increasing between 1.2 m and 2.0 m along the eastern and northeastern profiles, respectively (Fig. 7). These November 2012 and January 2013 storms were characterized by intervals of mean wind speed of ~5 m s^{-1}, lasting for a few hours, and ~6 m s^{-1} lasting for a day or more, respectively (Fig. 8). Within each of these specific winter storms there were a few hours-long episodes characterized by mean wind speed of ≥8 m s^{-1}. These mean conditions and hours-long wind bursts generated the storm waves; the more persistent the high-speed wind is, the higher are the instantaneous and mean waves (Fig. 8). The erosional impact of the November 2012 and January 2013 storms on the Nahal Darga delta, under the parallel coastal retreat was captured by TLS scans and revealed 2.3 and 3.0 m^3/m of erosion (i.e., eroded volume per meter length of the 50-m-long coast that was scanned), respectively (Figs. 7D and 8).

TLS data for the slightly sloping, silty mudflats located ~2 km south of the Nahal Darga site, acquired in April and May 2012, documented the formation of a small, 0.5-m-high step and ~2.5-m retreat (Fig. 7B). At the beginning of the following winter (November 2012), the LiDAR scan (Fig. 7) revealed ~2 m of additional lateral erosion and the formation of a new, but minor, 0.2-m high step. It formed at a lower elevation than the base of the May 2012 cliff. Finally, the January 2013 scan revealed an additional ~0.5-m of lateral erosion of the November 2012 cliff while the cliff height remained the same.

The observations of lake level, wind speed, and wave amplitudes during the 2012–2013 TLS measurements (Figs. 7 and 8) indicated that only a few winter windstorms are associated with coastal cliff formation. Therefore, infrequent storms, characterized by relatively high wind speeds that last up to a few days are identified as the cliff-forming storms. This raises the question on onshore erosion during summer.

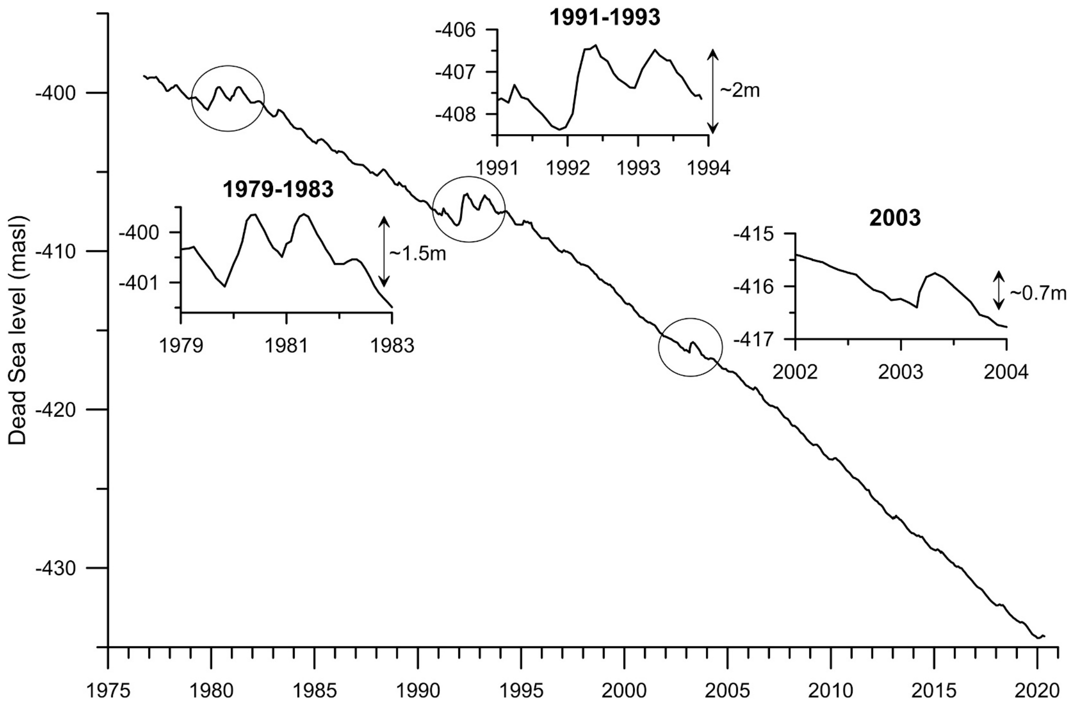

Fig. 9. Three pronounced (≥0.7 m) seasonal/annual lake level rises during the intervals of 1979–1980, 1991–1993, and 2007.

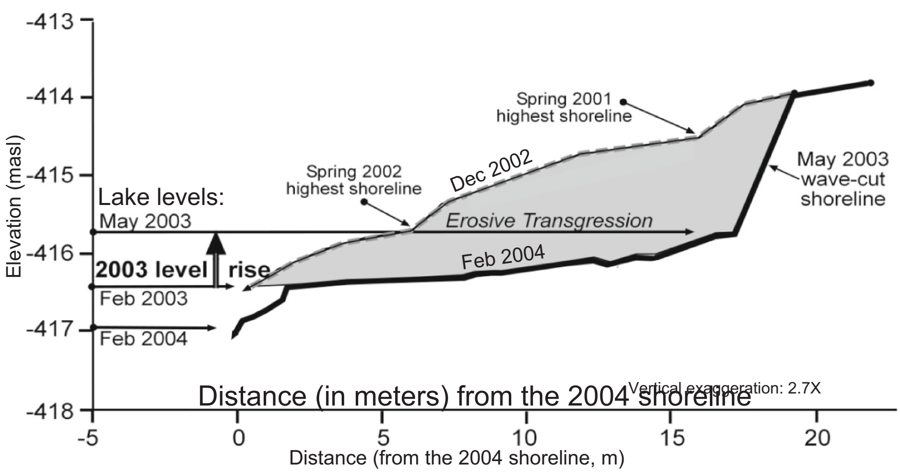

Fig. 10. An approximately 17-m long, inland transgressive erosion at a Dead Sea shore during the 0.7-m lake-level rise of February 2003. The topography (dashed line) measured in both 2001 and in January 2003 is of the shore profile staircase before the lake level rose a month later. The exact dates of the lake-level rise is uncertain, but it occurred within less than a month sometimes in February 2003. This rise caused erosional transgression and formed a ca. 2-m high cliff. A total volume of ~17 m^3 of mudflat sediments was removed per each 1 m of shore length (represented by the grey area, calculated as a triangle). In many places, this removed the shorelines of 2001 and 2002. Note that after May 2003, the lake level resumed falling and when the storms of the following winter (2003–2004) impacted the mudflats, the level was already lower and the wave-cut of 2003 was left unmodified above reach of the waves. The 2003 wave-cut cliff can currently be seen almost along the entire western shore of the Dead Sea. (For interpretation of the references to color in this figure legend, the reader is referred to the web version of this article.)

4.2. *Summer: regressive shore without cliff formation*

In contrast with the minor level rise or stability during winters, summers experience lake level falls because of the lack of inflow, high summer evaporation, and pumping of lake water for industrial use (Hamdani et al., 2018). This results in shoreline regression.

Summers experience an average wind speed of ~3 m s^{-1}, much weaker than the mean of 6 m s^{-1} with hours-long bursts of ≥8 m s^{-1} during the winter storms (Section 4.1); therefore, during the summer the lake is calmer and the waves are lower in amplitude (Fig. 8). Occasionally, summer winds do reach ~10 m s^{-1}; but these wind episodes last for only very short intervals, much shorter than the days-long persistent winter storms (Hamdani et al., 2018; Lensky et al., 2018). Our observations indicate that the associated summer storm waves (Fig. 8) have negligible impact on the coastline.

During the summer months of 2012, the TLS data at the abovementioned sites indicated a level fall and regressed coastline (Fig. 7) and an abandonment of the April–May 2012 cliff; indicating that the cliff was not impacted again by wave activity. The TLS surveys also indicated that during the summer of 2012, changes in the inshore topography were practically undetectable (Fig. 7). During the summer of 2013, following the above mentioned 2012–2013 winter storms, the coastline regression was faster than during the winter and, more importantly, without any observed erosion. Without additional windstorm-generated waves that impacted the base of the cliff during the rest of the winter (e.g., the wind of February 2013 in Fig. 8), the cliff of 2013 achieved its final form during the January 2013 storm. Later in 2013, this cliff was completely abandoned to become an additional step in the well-preserved regressive staircase sequence of the Dead Sea shores.

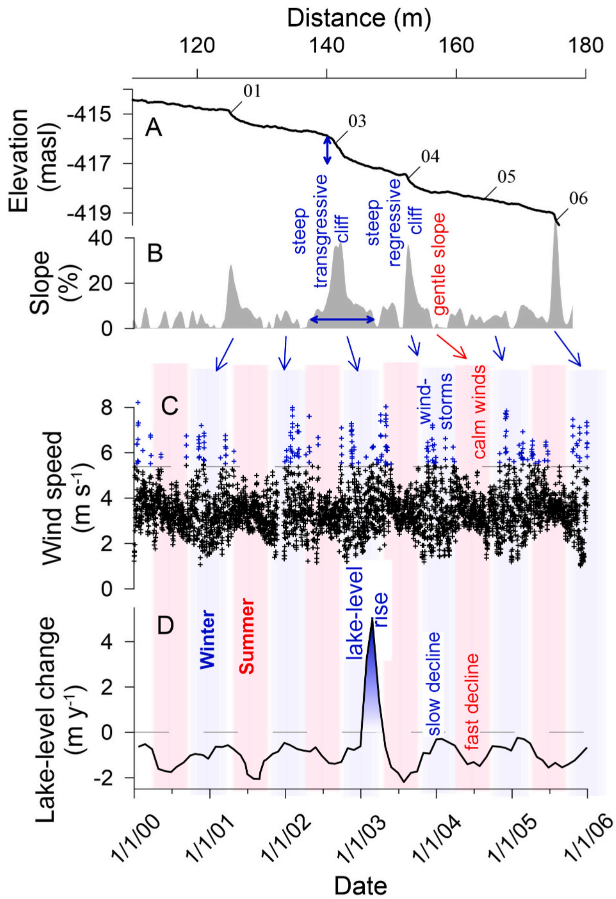

Fig. 11. (A) A topographic profile and (B) its derived slope across the studied mudflat showing the cliff/steps in the landscape (note that the 2003 cliff, marked as 03, has truncated the 2002 cliff). The arrows below panel B, connect the topography with the forming storms portrayed in (C) by high values (>6 m s^{-1}) in mean daily wind speed during winters and slower (usually <4 m s^{-1}) calm winds during summers. (D) The respective rates of the lake-level changes showing the relative slow decline of lake levels during winters and the faster lake-level decline during summers. A high rate (~4–5 m yr^{-1}) of lake-level rise is associated with the ~0.7-m level rise of February 2003.

4.3. *Annual lake-level change, storminess, and resulting staircase morphology*

The observed association between the seasonality of the wind regime, wave amplitude, storm duration, and cliff formation (e.g., Figs. 6–8) indicates that seasonality strongly influences cliff formation. Since summer lake level continues to decline and force a regression without storm waves, each of the cliffs observed along the Dead Sea most likely was formed at the winter lake level. Winters experience lower net level fall and as a result, the storm waves are capable of operating throughout the season almost at the same level.

This pronounced seasonality (a) dictates the seasonal pace of cliff formation at vertical intervals similar to the magnitude of the annual lake-level fall (~1 m), (b) facilitates the well-documented cliff separation in the landscape as observed by detailed surveys and mapping, and (c) allows the abovementioned determination of the exact year of each cliff formation by matching topography with the detailed, monthly-measured lake-level curve.

5. Cliff formation during rising and transgressive lake level

Following the last two decades of additional and continuous increase in fresh-water diversion from the Dead Sea watershed, recent winters experience reduced water-level rises. The ~20 cm lake-level rises, which have characterized many of the winters of the late 20th century, are now quite rare and their common amplitudes are only a few centimeters (Fig. 1, See also Lensky and Dente, 2015; Bodzin et al., 2018). Lake-level falls during the summers continued at a similar pace, maintaining the quite-repeated vertical separation between steps. For example, during the cliff formation of January 2013, the lake level rose by 0.2 m. This small level rise, which now became quite rare, was the outcome of a rare incidence of increased discharge (>120 × 10^6 m^3) of the lower Jordan River into the lake (Lensky et al., 2013).

The relatively small (<20 cm), but common, winter lake-level rises are associated with minor seasonal transgressive erosion. However, the modern lake-level curve (Figs. 1 and 9) indicate a few rare, but larger seasonal level rises associated with more noticeable transgressions.

Three modern wave-cut cliffs stand out as higher than the regular ~1-m high common cliffs at the staircase morphology along the western coast of the Dead Sea. Each of these distinctly higher cliffs is related to >0.7-m lake-level rises (Fig. 9) of the last four decades (1980–2020). These higher-than-normal seasonal rises occurred during the very wet winters to early springs of 1979–1980, 1991–1992, and in 2003. They were characterized by different amplitudes and encountered different geometry of already emerged delta fronts and/or mudflats. We assembled available data to study the responses of the various shores and environments to these three level rises.

5.1. *1979–1980 lake-level rise over a generally low-gradient coast and minor staircase cliffs*

The significant ~1.5 m annual level rise of 1979–1980 (Fig. 9) had only a minor impact on most of the western shores of the Dead Sea. This is mainly because at that time, at the edges of alluvial fans, the shore environment was quite flat, characterized by coastal berms, beach ridges, and lagoons, and the steeper delta fronts were only beginning to emerge above the fast-falling water level, with only initial increased steepness following the exposure of the tips of delta fronts. Fig. 4, for example, indicates that in 1979–1980, the tip of the Nahal Darga delta front was already standing 4–5 m above the contemporary lake level. The rising level and the storm waves during this wet winter truncated this initially exposed delta front and formed the observed cliff (Fig. 4). The mudflats were still underwater, unexposed to coastal processes.

5.2. *1991–1992 & 1992–1993 lake-level rises – impacting the steep slopes of delta fronts*

The 1991–1992 level rise (Fig. 9) occurred, in part, by a rare water release from the Sea of Galilee through the Jordan River into the Dead Sea. This water release was forced by the risk of overflow from the Sea of Galilee as a result of extremely wet winter season that recorded highest rainfall in the 170-year long precipitation record at Jerusalem (Amiran, 1995; Enzel et al., 2003). In the following 30 years between 1991 and 2021, water was released only once in 2003 (see below), into the lower Jordan River, mainly from the Yarmouk River (Fig. 1). The wettest 1991–1992 winter experienced frequent exceptional days-long winter windstorms waves.

In the steep (~25–30°) delta fronts, the most pronounced wave-cut cliff was formed by the combined impact of two lake level rises of ~2.4 m and ~1.2 m, occurring in the consecutive wet winters of 1991–1992 and 1992–1993, respectively. During their separating summer of 1992, the lake level dropped by ~1 m (Fig. 9). At a few delta fronts, the height of the coastal cliff generated during these two wet and stormy years reached >4 m (e.g., Fig. 2A). Although we visited and measured the shore in Nahal Darga delta front during and following each of these two wet winters, currently, it would be impossible to map and separate the cliff into its two years of formation; they amalgamated by lateral (transgressive) erosion into a single feature mapped as 1991–1992 (or 1991–1993) cliff. These two level rises and storms in

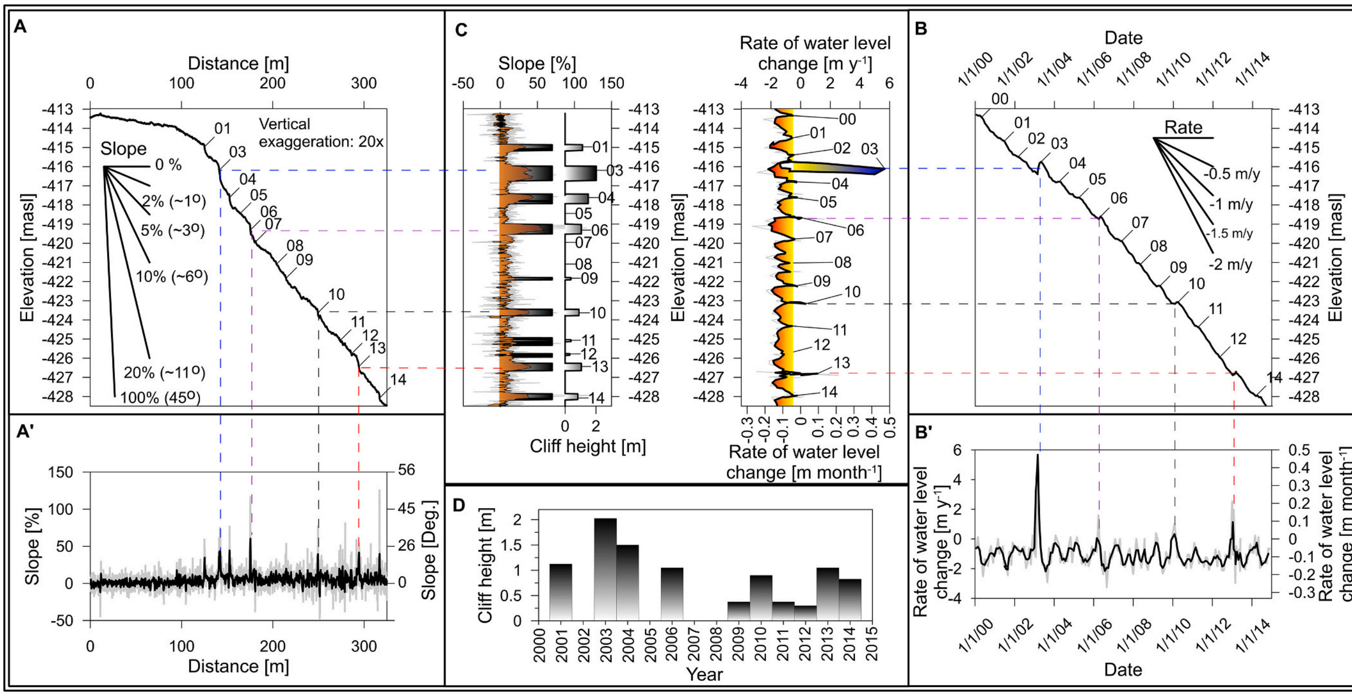

Fig. 12. Composite of topographic cross-sections, slopes (left side graphs), and the time series of the Dead Sea water level and the rate of level change (right side graphs). (A) Topographic profile (from Mineral Beach); (A′) Slope over distance (first derivative); (B) Dead Sea level; (B′) Rate of drop (or rise) of lake level (first derivative); (C) Rate of lake-level change and topographic slope projected against the topographic elevation (in order to correlate cliffs with lake-level rising); (D) Cliff height against cliff age. The independent lake level and topographic data have a common elevation axis, which enables exploring the relations between shoreline cliff formations (coastal erosion) and lake-level changes (hydrological changes). The slopes were calculated from the drone-based photogrammetry (5-cm resolution) across of the delta and mudflat cape. The derivative time series are plotted (grey curves) along with the three-points moving average smoothed plot (black curves). The slope and lake-level change rates are also projected to the elevation axis (two central graphs), assisting in the determination of the year of formation of each coastal cliff and associating cliff morphology to the rate of lake-level change. Specific years are marked (e.g., 2008 marked 08). The projections of four examples (2003, 2006, 2010, and 2013) are shown in dashed lines. Projecting the changing lake-level rate, driven by the regional seasonal hydroclimatology, to the elevation, results in the common loops for seasonal to annual lake-level rises (e.g., 2003).

subsequent years, and the substantial transgressive erosion in the delta front resulted in the highest cliff in the modern sequence of several deltas around the Dead Sea. Beach berm formed on coeval gentler alluvial fan surfaces (e.g., Fig. 2 and Bartov et al., 2006). The 1991–1992 level rise did not leave any erosional expression in most of the mudflats, because in the early 1990s they were still submerged and only their tops were beginning to emerge at few localities.

5.3. The 2003 cliff formation under abrupt lake-level rise and regular storms

The 2003 lake-level rise of 0.7 m (Fig. 9) resulted from a large discharge into the Dead Sea by water released in February 2003 from the Yarmouk River, the major tributary to the lower Jordan River, and less from the Sea of Galilee. The 2003 winter was exceptionally wet in the northern watershed of the Dead Sea, but less so in the area draining directly into the lake.

In the delta front, the 2003 lake-level rise produced a relatively high wave-cut cliff (Fig. 2A). This cliff is higher than the common, seasonal wave-cut cliffs forming in the delta-front under the ongoing regression (Section 4). In the mudflats, the height of the 2003 cliff is commonly ~2 m. At places, it reached 3–4 m (Fig. 2C), depending on the pre-existing topography encountered by the level rise and waves. During the 2003 late winter–early spring rise and regular winds, the steeper eastern edges of the mudflats already were exposed and an exceptionally large volume of fine-grained sediments (Figs. 10 and 2C), usually stored at the mudflats, was transported into the deep basin.

The 2003 cliff-forming event is the only example of a transgressive erosion at the mudflats during a rising lake level. Notably, this transgressive erosion occurred during regular winter windstorms (Fig. 11) such as the winds in 2012–2013 (Section 4 above). This connoted that abnormal lake-level rise (Fig. 9) can generate a pronounced lateral erosion even under common and regular winter hydroclimatology; i.e., wind storms drive the erosion. However, under a lake-level rise more frequent regular winds can amplify the cliff-forming erosive transgression.

6. The decadal-scale staircase morphology

6.1. Annual lake levels and staircase topography

To associate the formation of the stepped coastal morphology with the potential controlling mechanisms of lake-level fluctuations and storms, observed above, we converted the (a) topography of the cliff staircase, and (b) seasonal to annual lake levels into a common axis in Fig. 12. This allows better determination of the year of formation of each coastal cliff and, more importantly, to associate discrete cliffs in the staircase to a specific rate of level change. Fig. 12 presents the association between seasonal and annual lake levels and the morphologic expression of the many cliffs in the staircase. It connects the slope and elevation curves and emphasizes The heights and slopes of the cliffs. The recent changes in the lake-level rate are the first-order expression of the seasonality and variability of the regional hydroclimatology. Therefore, the closed connection of the lake level with the elevation of the staircase morphology, points to the role of the hydrometeorology in the Dead Sea watershed and storms in controlling the landforms.

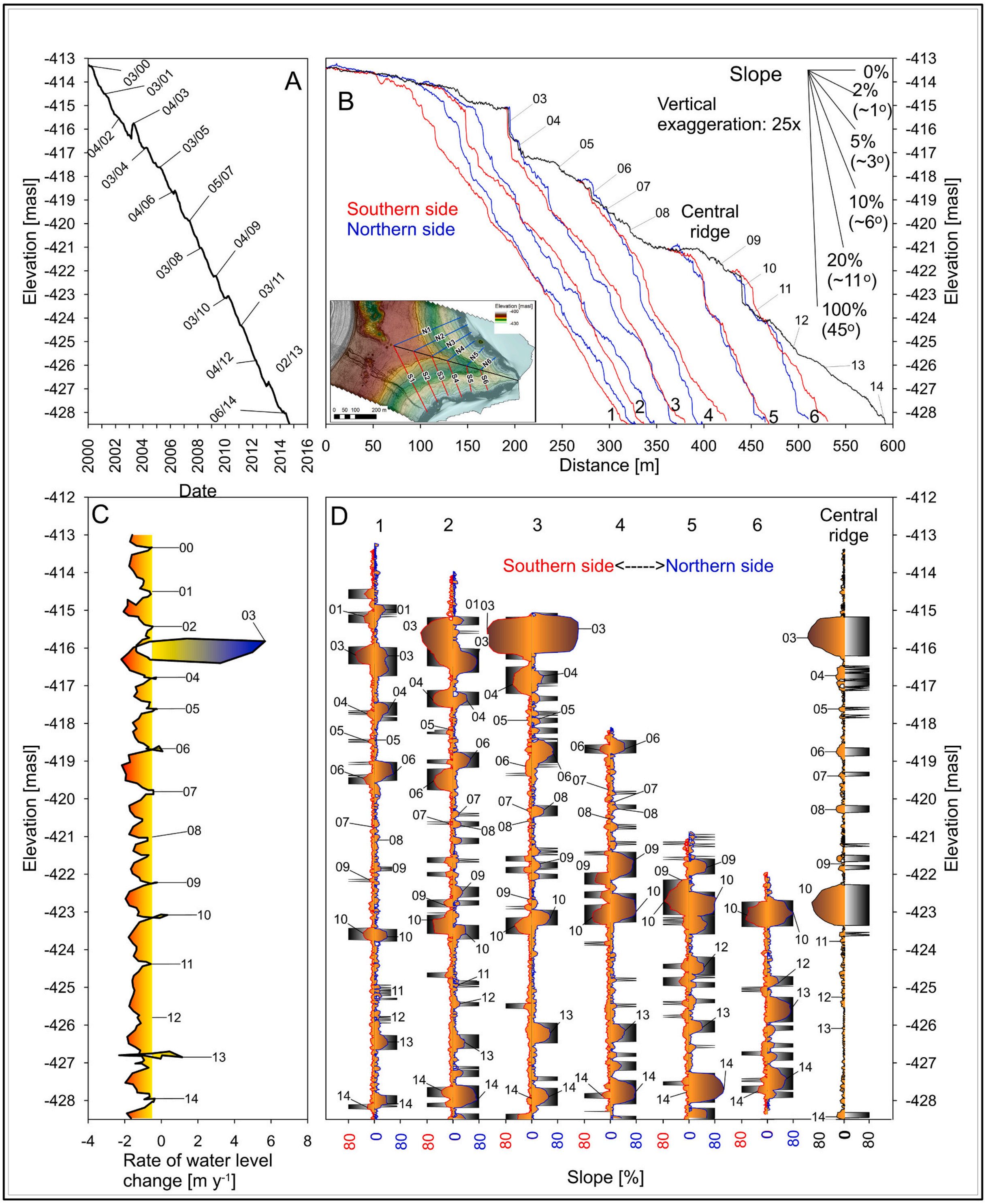

Fig. 13. The coastal cliff morphology of the Mineral Beach cape and the rate of lake-level change through time. (A) Time series of lake level. (B) Topographic transect profiles along a cape, see insert map for location. (C) The rate of change of lake level, positive rates are related to events of lake-level rise due to high winter inflows. (D) Slopes along the seven transects shown in (B). Note the same color-coding and numbering. Note the role of the lake-level rise in forming cliffs during the winters of 2003 and 2010 and that earlier lake-level rises are not documented here because this specific mudflat coast was still underwater.

6.2. Shore orientation

The topographic cross-sections of the Mineral Beach mudflat with its cape morphology, and of the Nahal Darga delta front (Figs. 13 and 14, respectively) indicate that cliff height slightly varies laterally, in part according to coast orientation or aspect, probably adding a secondary parameter. In addition, the delta front cross-sections face northeast, east, and southeast (Figs. 7 and 14) and cliff height and transgressions also show some lateral variability. The cross-sections of the Mineral Beach mudflat cape (Fig. 13) denote cliff heights that are larger at the nose of the cape relative to the more landward distal sides. In the world oceans such a lateral change is usually related to convergence of wave orthogonals. This may be the reason here as well, but we also observe that, with the reduced depth of the lake landward from the cape nose,

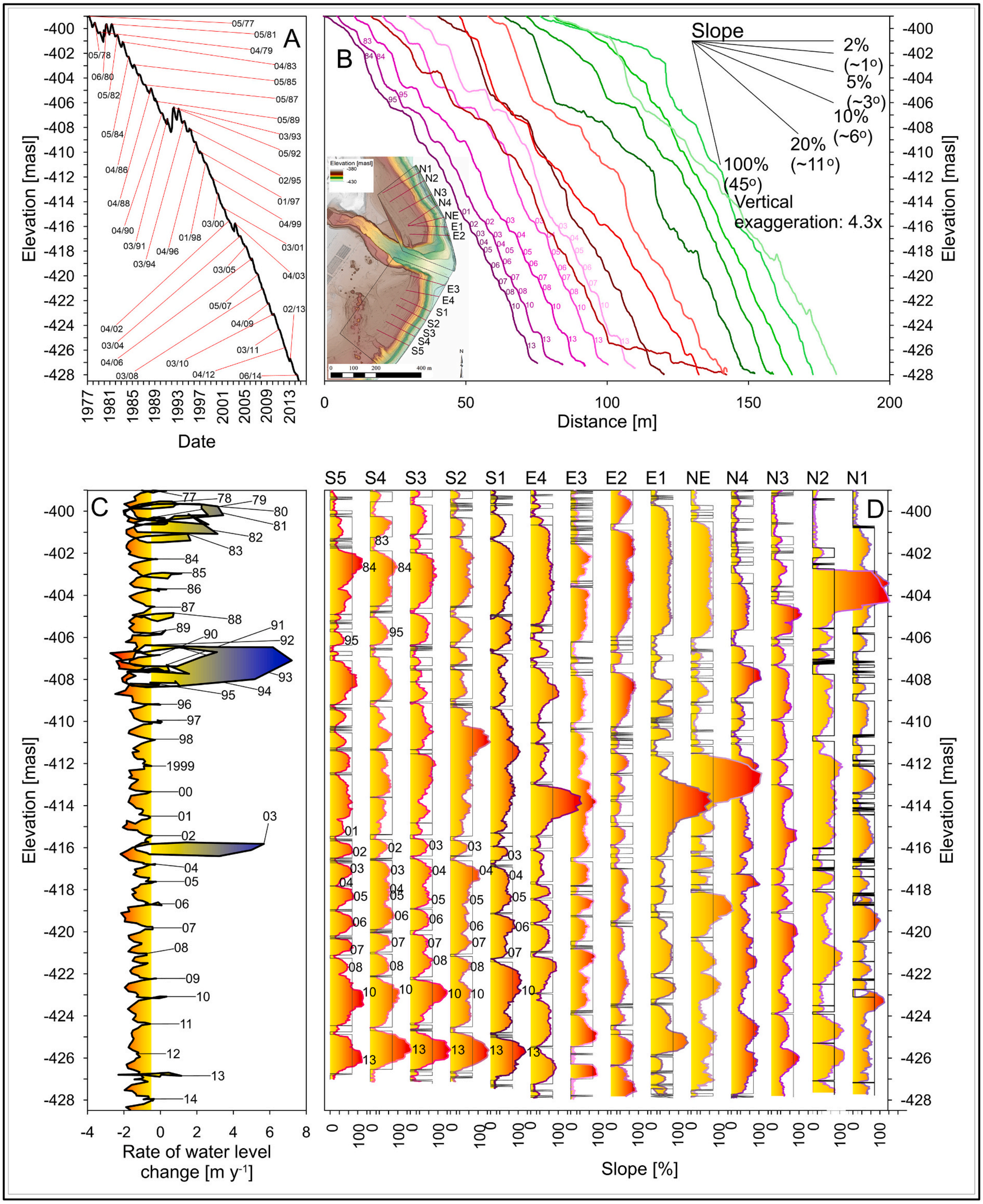

Fig. 14. The coastal cliff morphology of the delta front of Nahal Darga and the rate of level change through time. (A) Time series of lake level. (B) Topographic transect profiles across the delta front with respective lake levels during the years (e.g., 2003 marked as 03). (C) The rate of change of lake level, positive rates are related to events of lake-level rises due to high winter inflows. (D) Slopes along transects in (B) (N, NE, E, and S are the approximate direction of the profiles; see inset DTM map in (B) for location).

the aggressive waves attenuate westward. This, in turn, indicates that under stabilized lake level, the muddy capes will be eroded quite fast landward from east to west.

6.3. Coalescence

Both Figs. 13 and 14 document coalescence of cliffs from different years/lake stands. Cliff coalescence occurs when cliffs formed in a given year/winter or multiple years laterally retreat and obliterate older pre-existing higher-in-the-sequence cliffs. Coalescence becomes common

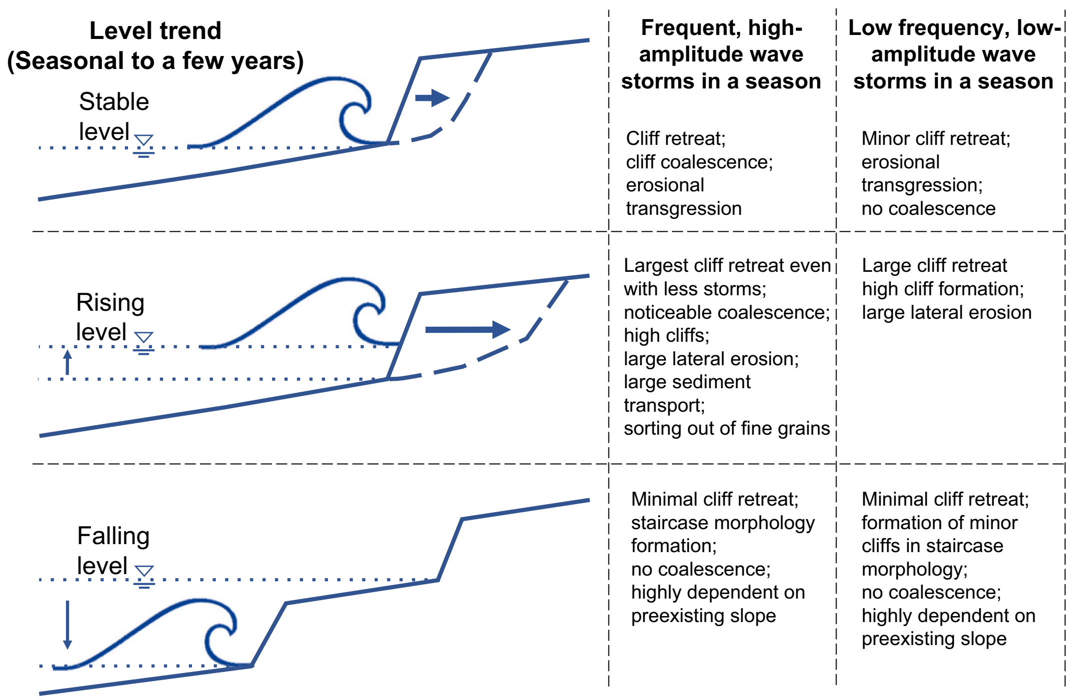

Fig. 15. A schematic view of the impact of falling, rising and stable Dead Sea levels on its stepped shore morphology. Stable and rising lake levels will laterally erode the shore even under regular winter windstorms. During stormy wet years the lateral erosion grows and is capable of reaching tens of meters inland.

under fluctuating lake levels and is pronounced when the level rises with the minimal amplitudes of the annual level fall. Therefore, the existance of coalescence in a staircase coastal morphology indicates a dynamic negative and positive lake-level change. Along the Dead Sea margins, under current environmental conditions, coalescence mainly indicates a forced regression punctuated by transgressive lake-level rises at the sub-seasonal to decadal (or even longer) temporal scales. Furthermore, existence of the coalesced cliffs points to the impact of windstorms and waves and the control of the sub-seasonal weather or multi-year hydrologic change.

An example for a common coalescence is the 2012–2013 retreat of cliff that reached the position of the cliff formed during the previous winter season of 2011–2012 and eroded it off at places (Fig. 7). In map view, we recognize two types of coalescence in the Dead Sea cliff staircase morphology: (a) a parallel-overriding coalescence, and (b) an angular to sub-parallel cross-cutting coalescence. Angular coalescence is easier to detect in the field and in airborne images; it indicates a lake-level rise following a regressive lake-level fall. An example is the remnants of a sub-seasonal cliff generated during the minor lake-level rise of January 2006 (Fig. 5B and Fig. S1). Another extreme example is the 2003 transgressive cliff (Section 5.3), which has overridden and eroded the 2002 cliff (Figs. 10, 5B, and Fig. S1). The 2003 cliff (Section 5.3; Figs. 2, 10, 11) coalesced with the 2002 and 2001 cliffs in the mudflats and at the tip of the Mineral Beach cape (Figs. 2, 5B, Fig. S1). Remnants of the 2001 cliff are represented in the northern (N1) and southern (S1) transects of Fig. 13 and Fig. S1.

7. Regional hydroclimatology enhancing cliff formation

Our results indicate that cliff retreat and associated largest lateral erosion along the Dead Sea shores are the product of combined lake-level rise and stormy weather during the winter seasons (Figs. 11–12). Winter is the rainy season in the northern and central parts of the Dead Sea watershed. Wetter-than-average winters can enforce the lake-level rises (Enzel et al., 2003; Enzel et al., 2008; Morin et al., 2019) because they are associated with seasonal increased frequency of eastern Mediterranean low-pressure systems. During the wettest winters, these systems are also deeper, move slower, and their tracks are at a 1–2° lower latitude across the eastern Mediterranean (Striem, 1974; Ben Dor et al., 2018; Enzel et al., 2003; Kushnir et al., 2017; Morin et al., 2019; Armon et al., 2018, 2019; Ziv et al., 2006). These systems bring >90% of the annual rains to the watershed; when seasonal to multi-year precipitation is significantly higher than the long-term mean, a lake rise is evident in the high and low-resolution records (Enzel et al., 2003; Ben Dor et al., 2018; Morin et al., 2019). Coevally, these winter precipitation in the northern watershed and lake-level rises, are associated with intervals characterized by persisting (or more frequent) high winds and highest waves in the Dead Sea. i.e., these systems explain why years with naturally rising levels are also windier in the Dead Sea; acting together, they amplify shore erosion. Embedded within this mean daily wind speed are persistent episodes of hours- to days-long intense winds ((Arnon et al., 2019; Gertman and Hecht, 2002; Hamdani et al., 2018) with instantaneous wind speed exceeding 12 m s^{-1}. These extended winter systems generate relatively long storm waves that last between several hours to a few days (Eyal et al., 2021). As shown above, these winds and waves are essential in eroding the lakeshore and forming the winter-cliff staircase morphology.

This synoptic- and regional-scale hydrometeorology controls both the lake-level rise and the waves. Therefore, the clear separation between these two cliff-generating causes is obscured. We stress that in this regard, the 2003 coastal-cliff evolution (Section 5.3) provides rare evidence that under a lake-level rise, which surpasses the common minor seasonal rises, regular winter windstorms and waves are sufficient to generate an exceptionally high cliff (Figs. 10, 11, 14). Usually, such a level rise occurs in years with several such eastern Mediterranean storms.

8. Lessons from the modern coastal cliffs

8.1. The transience of mudflats and deltas

Currently, extensive mudflats and deltas exist along the western margins of the Dead Sea. What would remain of them in the Quaternary geological record? In this regard, the widespread remnants of the Late

Pleistocene (and some earlier) coarse-clastic deltas may be due to the relatively fast rate of Lake Lisan drop to its much lower Dead Sea levels (Bartov et al., 2003; Torfstein and Enzel, 2017), without the lake level reaching these, and the intermediate, stands since.

Remnants of pre-modern mudflats are less common along the Dead Sea margins (e.g., Bartov et al., 2007). The western Dead Sea mudflats represent a small portion of the suspended load that arrives with the flash floods adding annually only a mm- to cm-scale layer to them (e.g., Bartov et al., 2006); the majority of the suspended load spread across its deep basin (Bartov et al., 2006; Nehorai et al., 2013). Therefore, rebuilding a mudflat, following erosion by storms, is relatively a long process; based on available chronology (e.g., Enzel et al., 2000) these are centuries-scale features.

When waves, under natural, pre-regulation level rises interacted with the soft muddy or unconsolidated gravely sediments at the Dead Sea shores, truncation of the preexisting topography was and is quite efficient. This is a characteristic of the structurally controlled steep topography of the eastern edge of the deltas of the northern Dead Sea.

Our decadal-scale observations provide a crucial insight: Rising (and stable) lake levels do not simply flood or climb on top of the preexisting topography, which practically is the topography (or bathymetry) the lake has regressed on and marked it with the staircase morphology. A transgressive lake-level rise, or even stabilizing lake level, truncates almost horizontally inland the preexisting topography (e.g., Figs. 10 and 15), a phenomenon currently more pronounced at steeper delta fronts and eastern edges of the mudflats. Under transgressive lake-level rise, lateral erosion is more aggressive and forms a relatively wide platform; in the abovementioned example, the ~0.7-m 2003 rise has produced 17 m of lateral, relatively flat transgressive truncation, within a month or less according to data resolution (Fig. 10). As this process truncates at the base of the forming cliff, it has formed a cliff 3–6 times higher than the magnitude of the actual lake-level rising. i.e., the wider is the transgression inland and its associated level rise, the higher is the resulted transgressive wave-cut cliff and the erosional coastal platform. This also indicates the efficiency in removing coastal sediments from both the delta fronts and the mudflats into the abutting and accommodating deep lake.

We propose that the only reason current mudflats are so extensive is the forced regression, which follows the rapid anthropogenic-induced, lake-level decline. Under natural, decimeters to meters up-and-down annual lake-level fluctuations, mudflats would have been rapidly removed by the almost constant action of storm waves at the similar level at their eastern edges, leaving behind only small remains, such as observed in the Quaternary stratigraphic record of the Dead Sea.

At the delta fronts, repeated truncations, under stable or rising lake level with magnitudes similar to 1980, 1992, or 2003 (Section 5), would have generated a noticeable ravinement, an erosional surface observed in the coarse-clastic stratigraphy of several of the Dead Sea Late Pleistocene and Holocene deltas (Bowman, 1971; Enzel et al., 2000; Bartov et al., 2007, 2012).

8.2. Implications to the planned Red-Dead project and current infrastructure

The Red-Dead Project is the largest proposed regional development initiative in the Middle East. An objective of this initiative is to either moderate the rate of the anthropogenic Dead Sea level decline or even stabilizing the lake level (Gavrieli et al., 2011). The above lessons from the anthropogenically-induced lack of seasonal rises have profound implications for understanding the fate of the Dead Sea shores under longer-term lake-level stabilization.

Stable lake levels, even without seasonal rising, maintain coastal erosion for years to decades at similar levels. One of the main lessons from this research is that stabilized levels allow the storm waves to impact repeatedly and for a longer duration the specific shore height during individual or a sequence of wet and regular winters. This may have harsh consequences. As the infrastructure along most of the western coastal zone of the Dead Sea is located only hundreds of meters from the current and future shores, we anticipate two potentially devastating impacts, probably acting together. (a) A direct and accelerated lateral coastal erosion, due to the longer-duration vertical stability of the shore height, will quickly further narrow the already slender coastal zone. (b) As we observed in 1992–1993 and 2003–2004, with the lateraly retreating shore, tributary stream incisions (Ben Moshe et al., 2008; Eyal et al., 2019; Dente et al., 2021) will accelerate. This increased incision near the shore, is the outcome of the shortening of the stream profile on quite a stable base level. The cliff retreat would drastically increase the stream gradients near the stream mouth and this gradient would propagate upstream either through a diffusive, gradient-dependent incision or a parallel knickpoint retreat. This upstream propagation of stream gradient would undermine the main highway, bridges, and other installations along the Dead Sea shores. Stream mouths with an emerging steep bathymetry in front of them will allow transfer of the incision products to the deep basin. Such stream mouth bathymetries will not allow the development of deltas, which may have the capacity to moderate the incision (e.g., Dente et al., 2017). We predict that even a small magnitude artificial lake-level rise or stabilization, will have repeated and therefore, an amplified impact on lateral erosion, much larger than the near instantaneous 2003 erosion (Section 5.3).

8.3. Implications to other global cliffed coasts

Although we view the Dead Sea staircase morphology as a potential natural experiment of cliff formation, we are aware that there are differences in the actual processes, rates, and magnitudes between these cliffs and the cliffs around the world's seas and oceans; e.g., bedrock vs. soft sediment, wave amplitudes, duration of storm action, cliff heights and collapses, and rates of sea level changes. However, as laboratory experiments assisted in detecting controls over coastal erosion, the up-scaled natural experiments the Dead Sea setting provides, at the field scale, are useful at least in viewing the process operating at the field scale. Furthermore, there are also some distinct similarities between these lacustrine and ocean coastal environments, even if the level changes are very different (e.g., Garcia et al., 2021). As in the Dead Sea, cliff erosion has been related, among other controls, to wave action, beach geometry, and cliff lithology (e.g., Young et al., 2021); these parameters are the drivers in the Dead Sea, as waves operate on the pre-existing topography of the unconsolidated lithologies.

When measuring hazardous retreats along the global cliff coasts, studies focus on late Holocene and modern cliffs; they point to the impact of storms (e.g., Mushkin et al., 2016, 2019), slides and collapses, and on the dependency on the local stratigraphy and bedrock lithology. Others document cliffs that have been formed during earlier interglacials. In practice, they document remnants of the geomorphic expression of related platforms and terraced cliff shores at eustatic glacial-interglacial scales. In places, these long-term landforms are tectonically uplifted and therefore observed above the current interglacial high stand. Together with coastal erosion they leave, above current sea level, a landscape of staircase-like sequences of fossil ancient coastal landforms, mainly related to earlier interglacial high stands (Pedoja et al., 2014; Muhs et al., 1994, 2020). Such staircase sequences are difficult to date and only a few are reported in detail from around the world. As a result, examples of coasts characterized by one or two well-studied shores and their respective lateral erosion are limited. However, as identified by Harvey et al. (1999) and Mackey et al. (2014), the erosion associated with such coastal cliffs and their landward retreat during higher interglacial sea levels, which underlie staircase sequence formation, can have a profound impact on inland landscapes through the upstream propagation of stream profiles as will occur and projected for the Dead Sea shores.

9. Conclusions

The modern, Dead Sea coastal cliff staircase, surveyed and mapped at high resolution, and the individual sub-seasonal cliff erosion supported by wind and wave data, indicate that individual winter storms generate these cliffs under consecutive regressive and transgressive lake-level fall and rise. Winter storm waves control over the regularity of the shore morphology and seasonal (mostly summer) lake-level falls explain the common heights of the steps in the resulted staircase morphology. Cliffs do not form during the summers as they lack sufficient windstorms. The up-to-a-few-days-long winter windstorms are generated by the passage of eastern Mediterranean low-pressure systems. Increased frequency of such storms during individual winters or clusters of winters, potentially raises lake level and generates wind and waves at the Dead Sea. The quite regular ~1 m steps of the staircase morphology are caused by erosion during winter storms and by the ~1 m annual lake level fall, which is primarily controlled by summer evaporation and lack of windstorms. As a result, the staircase morphology manifests the close control of the synoptic-scale climatology on the hydrology, wind, and waves of the lake basin.

It is difficult to separate the effect of winter rain, inflow, and lake rising from the winter windstorms. However, hydrologically-controlled lake-level changes without wind or storm waves are incapable of forming the coastal cliffs. Any transgressive erosion during regular winters or anomalously wet winters is always associated with windstorms. Rising lake levels alone seem ineffective in generating cliffs. The rare, relatively large, lake-level rises produced the highest cliffs and terraces in the coastal profile. Geometrically, the steepness of the exposed coarse clastic delta fronts and the steeper frontal (eastern) edges of the mudflats accelerate the impact of erosion. A lake-level rise, associated with weak to moderate storms generates a cliff. Sustained lake-level rise together with increased frequency and magnitude of seasonal storm waves, would have a major impact on the Dead Sea shores. Combined, they would generate much larger transgressive erosion, a higher and faster landward migration of wave-cut cliffs, erosion of large volumes of sediments, and generation of a pronounced ravinement that can threaten infrastructure along the coast of the lake.

Supplementary data to this article can be found online at https://doi.org/10.1016/j.geomorph.2022.108237.

Declaration of competing interest

All authors do not have a conflict of interests.

Acknowledgement

We thanks L. Ben Moshe and Y. Bartov for the topographic surveys of the 2003 erosion used in Fig. 10 and the many students over the last 30 years who helped generating some of the observational data. We appreciate the detailed review by three unknown reviewers and the editor, which improved the presentation of the content and readability of earlier versions of the manuscript. This study was funded by the Israel Science Foundation grants 946/18 (to YE) and 1471/18 (to NGL), United States-Israel BSF grants 2018/035 and 2019/637 to NGL, and by the Israeli Government under the Geological Survey of Israel, Dead Sea Project (PI AM). HE is thankful for the Azrieli Foundation and the Pfeifer Family fellowships.

References

Abu Ghazleh, S., Kempe, S., 2009. Geomorphology of Lake Lisan terraces along the eastern coast of the Dead Sea, Jordan. Geomorphology 108, 246–263.

Abu Ghazleh, S., Abed, A.M., Kempe, S., 2011. The dramatic drop of the Dead Sea: background, rates, impacts and solutions. In: Badescu, V., Cathcart, R.B. (Eds.), Macro-engineering Seawater in Unique Environments, Environmental Science and Engineering. Springer-Verlag, Berlin, pp. 77–105.

Amiran, D.H.K., 1995. Climatic Data for Jerusalem. Jerusalem Institute For Israel Studies, Jerusalem, 141 p.

Armon, M., Dente, E., Smith, J.A., Enzel, Y., Morin, E., 2018. Synoptic-scale control over modern rainfall and flood patterns in the Levant drylands with implications for past climates. J. Hydrometeorol. 19, 1077–1096.

Armon, M., Morin, E., Enzel, Y., 2019. Modern atmospheric patterns controlling rainfall and floods into the Dead Sea: implications to the lake's sedimentology and paleohydrology. Quat. Sci. Rev. 216, 58–73.

Arnon, A., Lensky, N.G., Selker, J.S., 2014. High-resolution temperature sensing in the Dead Sea using fiber optics. Water Resour. Res. 50, 1756–1772. https://doi.org/10.1002/2013WR014935.

Arnon, A., Selker, J.S., Lensky, N.G., 2016. Thermohaline stratification and double diffusion diapycnal fluxes in the hypersaline Dead Sea. Limnol. Oceanogr. 61, 1214–1231.

Arnon, A., Brenner, S., Selker, J.S., Gertman, I., Lensky, N.G., 2019. Seasonal dynamics of internal waves governed by stratification stability and wind: Analysis of high-resolution observations from the Dead Sea. Limnol. Oceanogr. 64, 1864–1882.

Barnard, P.L., van Ormondt, M.E., Li, H., et al., 2014. Development of the Coastal storm Modeling System (CoSMoS) for predicting the impact of storms on high-energy, active-margin coasts. Nat. Hazards 74, 1095–1125.

Bartov, Y., Stein, M., Enzel, Y., Agnon, A., Reches, Z., 2002. Lake levels and sequence stratigraphy of Lake Lisan, the late Pleistocene precursor of the Dead Sea. Quat. Res. 57, 9–21.

Bartov, Y., Goldstein, S.L., Stein, M., Enzel, Y., 2003. Catastrophic arid events in the East Mediterranean linked with the North Atlantic Heinrich events. Geology 31, 439–442.

Bartov, Y., Bookman, R., Enzel, Y., 2006. Current depositional environments at the Dead Sea margins as indicators of its past levels. In: Enzel, Agnon, Y., Stein, M. (Eds.), New Frontiers in Dead Sea Paleoenvironmental Research, 401. Geological Society of America Special Paper, pp. 127–140.

Bartov, Y., Enzel, Y., Porat, N., Stein, M., 2007. Sequence stratigraphy and lake-level reconstruction techniques: example from the Pleistocene-Holocene Dead Sea basin. J. Sediment. Res. 67, 680–692.

Bartov, Y., Stein, M., Enzel, Y., Kendell, C., Moore, P., 2012. Modeling the sensitivity to environmental controls of the Late Pleistocene lacustrine delta sequences in the Dead Sea basin. In: Baganz, O.W., Bartov, Y., Bohacs, K., Nummedal, D. (Eds.), Lacustrine Sandstone Reservoirs and Hydrocarbon Systems: AAPG Memoir, 95, pp. 417–431.

Ben Dor, Y., Armon, M., Ahlborn, M., Morin, E., Erel, Y., Brauer, A., Schwab, M.J., Tjallingii, R., Enzel, Y., 2018. Drastic changes in winter flood frequencies in the eastern Mediterranean-Levant under drier vs wetter late Pleistocene eastern Mediterranean climates. Sci. Rep. 8 (8445), 1–4.

Ben Moshe, L., Haviv, I., Enzel, Y., Zilberman, E., Matmon, A., 2008. Basin hydrology and sediment diffusion modeling of incising alluvial streams under the fast falling base level of the Dead Sea, Israel. Geomorphology 93, 524–536.

Ben-Moshe, L., 2006. Longitudinal Profiles of Alluvial Streams in Response to Twentieth Century Changes in Dead Sea Level, Report GSI/02/06. Geological Survey of Israel, Jerusalem, Israel. https://www.gov.il/BlobFolder/reports/ben-moshe-report-2016/he/report_2006_GSI-02-2006.pdf, 142 p.

Bodzin, R., Lensky, N., Lutzky, H., Arnon, A., 2018. Dead Sea level: high resolution observations and their significance. Geological Survey of Israel. https://www.gov.il/en/departments/publications/reports/bodzin-et-al-poster.

Bookman, R., Bartov, Y., Enzel, Y., Stein, M., 2006. The levels of the late Quaternary lakes in the Dead Sea basin: a two centuries of research. In: Enzel, Y. Agnon, Stein, M. (Eds.), New Frontiers in Dead Sea Paleoenvironmental Research, 401. Geological Society of America Special Paper, pp. 155–170.

Bowman, D., 1971. Geomorphology of the shore terraces of the late Pleistocene Lisan lake (Israel). Palaeogeogr. Palaeoclimatol. Palaeoecol. 9, 183–209.

Bowman, D., 1997. Geomorphology of the Dead Sea western margins. In: In Niemi, T.M., Ben-Avraham, Z., Gat, J.R. (Eds.), The Dead Sea: The Lake and its Setting. Oxford University Press, Oxford, UK, pp. 217–225.

Bowman, D., Banet-Davidovich, D., Bruins, H.J., Van der Plicht, J., 2000. Dead Sea shoreline facies with seismically-induced soft-sediment deformation structures, Israel. Isr. J. Earth Sci. 49, 197–214.

Bray, M.J., Hooke, J.M., 1997. Prediction of soft-cliff retreat with accelerating sea level. J. Coast. Res. 13, 453–467.

Collins, B.D., Sitar, N., 2008. Processes of coastal bluff erosion in weakly lithified sands, Pacifica, California, USA. Geomorphology 97, 483–501.

Dawson, R.J., Dickson, M.E., Nicholls, R.J., Hall, J.W., Walkden, M.J.A., Stansby, P.K., Mokrech, M., Richards, J., Zhou, J., Milligan, J., Jordan, A., Pearson, S., Rees, J., Bates, P.D., Koukoulas, S., Watkinson, A.R., 2009. Integrated analysis of risks of coastal flooding and cliff erosion under scenarios of long term change. Clim. Chang. 95, 249–288.

Dente, E., Lensky, E., Morin, E., Grodek, T., Sheffer, N., Enzel, Y., 2017. Geomorphic response of a long channel to modern, decades-long, continuous base-level lowering: Nahal HaArava, the Dead Sea. J. Geophys. Res. Earth Surf. 122, 2468–2487.

Dente, E., Lensky, N.G., Morin, E., Enzel, Y., 2021. From straight to deeply incised meandering channels: slope impact on sinuosity of confined streams. Earth Surf. Process. Landf. 1–14.

Dickson, M.E., Walkden, M.J.A., Hall, J.W., 2007. Systematic impacts of climate change on an eroding coastal region over the twenty-first century. Clim. Chang. 84, 141–166.

Emery, K., Kuhn, G., 1982. Sea cliffs: their processes, profiles, and classification. Geol. Soc. Am. Bull. 93, 644–654.

Enzel, Y., Bar-Yosef, O., 2017. Quaternary of The Levant, Environments, Climate Change, and Humans. Cambridge University Press, Cambridge, UK, p. 771 p.

Enzel, Y., Kadan, G., Eyal, Y., 2000. Holocene earthquakes in the Dead Sea graben from a fan-delta sequence. Quat. Res. 53, 34–48.

Enzel, Y., Ken-Tor, R., Sharon, D., Gvirtzman, H., Dayan, U., Ziv, B., Stein, 2003. Late Holocene climates of the near East deduced from Dead Sea level variations and regional winter rainfall. Quat. Res. 60, 263–273.
Enzel, Y., Agnon, A., Stein, M., 2006. New Frontiers in Dead Sea Paleoenvironmental Research. Special Paper 401. The Geological Society of America, Boulder, Colorado, pp. 1–253.
Enzel, Y., Amit, R., Dayan, U., Crouvi, O., Kahana, R., Ziv, B., Sharon, D., 2008. The climatic and physiographic controls of the Eastern Mediterranean over the late Pleistocene climates in the southern Levant and its neighboring deserts. Glob. Planet. Chang. 60, 165–192.
Eyal, H., Dente, E., Haviv, I., Enzel, Y., Dunne, T., Lensky, N.G., 2019. Fluvial incision and coarse gravel redistribution across the modern Dead Sea shelf as a result of base-level fall. Earth Surf. Process. Landf. 44, 2170–2185.
Eyal, H., Enzel, Y., Meiburg, E., Vowinckel, B., Lensky, N.G., 2021. How does coastal gravel get sorted under stormy longshore transport? Geophys. Res. Lett. 48 (21), e2021GL095082 https://doi.org/10.1029/2021GL095082.
Garcia, F.-J., Morales, J.-A., Castañeda, C., Plomaritis, T.A., 2021. Shallow lacustrine versus open ocean coastal clastic deposits: Morphosedimentary diagnostic indicators and interpretation. Sediment. Geol. 423 https://doi.org/10.1016/j.sedgeo.2021.105981.
Gavrieli, I., Lensky, N., Abelson, M., Ganor, J., Aharon, O., Brenner, S., Lensky, I., Shalev, E., Yechieli, Y., Dvorkin, Y., Gertman, I., Scott, W., Ehud, S., Reznik, I., 2011. Red Sea to Dead Sea Water Conveyance (RSDSC) Study: Dead Sea Research Team. Report Number: GSI/10/2011 and Tahal Group. Jerusalem: Geological Survey of Israel. https://doi.org/10.13140/RG.2.2.24893.72164.
Gertman, I., Hecht, A., 2002. The Dead Sea hydrography from 1992 to 2000. J. Mar. Syst. 35, 169–181.
Groisman, M., 2013. Regressive and Transgressive Coastal Erosion by Waves and Short-duration Modern Dead Sea Lake-level Rises. Can be downloaded. The Hebrew University of Jerusalem. http://arad.mscc.huji.ac.il/dissertations/H/JSL/001925974.pdf.
Hackney, C., Darby, S.E., Leyland, J., 2013. Modelling the response of soft cliffs to climate change: a statistical, process-response model using accumulated excess energy. Geomorphology 187, 108–121.
Hall, J.W., Meadowcroft, I.C., Lee, E.M., van Gelderd, P.H.A.J.M., 2002. Stochastic simulation of episodic soft coastal cliff recession. Coast. Eng. 46, 159–174.
Hamdani, I., Assouline, S., Tanny, J., Lensky, I.M., Gertman, I., Mor, Z., Lensky, N.G., 2018. Seasonal and diurnal evaporationfrom a deep hypersaline lake: the Dead Sea as a case study. J. Hydrol. 562, 155–167.
Harvey, A.M., Silva, P.G., Mather, A.E., Goyd, J.L., Stokes, M., Zazo, C., 1999. The impact of Quaternary Sea-level and climatic change on coastal alluvial fans in the Cabo de Gata ranges, Southeast Spain. Geomorphology 28, 1–22.
Huppert, K.L., Perron, J.T., Ashton, A.D., 2020. The influence of wave power on bedrock sea-cliff erosion in the Hawaiian Islands. Geology 48, 499–503.
Hurst, M.D., Rood, D.H., Ellis, M.A., Anderson, R.S., Dornbusch, U., 2016. Recent acceleration in coastal cliff retreat on the south coast of Great Britain. Proc. Natl. Acad. Sci. U. S. A. 113, 13336–13341.
Israel Hydrological Service, 2015. Dead Sea Levels 1976-2015, Annual Reports, Israel Hydrological Service, Water Authority, Israel.
Jewell, P.W., 2016. Quantitative identification of erosional Lake Bonneville shorelines, Utah. Geomorphology 253, 135–145.
Katz, O., Mushkin, A., 2013. Characteristics of sea-cliff erosion induced by a strong winter storm in the eastern Mediterranean. Quat. Res. 80, 20–32.
Krueger, R., Zoet, L.K., Rawling, J.E.I.I.I., 2020. Coastal bluff evolution in response to a rapid rise in surface water level. J. Geophys. Res. Earth Surf. 125, e2019JF005428.
Kushnir, Y., Dayan, U., Ziv, B., Morin, E., Enzel, Y., 2017. Climate of the Levant: phenomena and mechanisms. In: Enzel, Y., Bar-Yosef, O. (Eds.), Quaternary of the Levant: Environments, Climate Change, and Humans. Cambridge University Press, Cambridge, UK, pp. 31–44.
Le Cossec, J., Duperret, A., Vendeville, B.C., Taibi, S., 2011. Numerical and physical modelling of coastal Cliff retreat processes between La Heve and Antifer capes, Normandy (NW France). Tectonophysics 510, 104–123.
Lensky, N., Dente, E., 2015. The Causes for Accelerated Recession Rate of the Dead Sea. Geological Survey of Israel Report GSI/16/2015. Special Publication. https://doi.org/10.13140/RG.2.2.20318.56641, 378 p.
Lensky, N.G., Dvorkin, Y., Laykhovsky, V., Gertma, I., Gavrieli, I., 2005. Water, salt, and energy balances of the Dead Sea. Water Resources Research 41 (12), 1–13, 2005WR004084.
Lensky, N.G., Gertman, I., Arnon, A., Ozer, T., Biton, E., Katsenelson, B., Bodzin, R., 2013. Currents and Hydrography of the Dead Sea: A Study for the Salt Recovery Project. Geological Survey of Israel Rep. No. GSI/20/2013, 31 p. https://www.gov.il/BlobFolder/reports/lensky-et-al-report-2013-21/he/report_2013_GSI-21-2013.pdf.
Lensky, N.G., Lensky, I.M., Peretz, A., Gertman, I., Tanny, J., Assouline, S., 2018. Diurnal course of evaporation from the Dead Sea in summer: A distinct double peak induced by solar radiation and night sea breeze. Water Resources Research 54, 150–160. https://doi.org/10.1002/2017WR021536.
Mackey, B.H., Scheingross, J.S., Lamb, M.P., Farley, K.A., 2014. Knickpoint formation, rapid propagation, and landscape response following coastal cliff retreat at the last interglacial sea-level highstand: Kaua'i, Hawai'i. Geol. Soc. Am. Bull. 126, 925–942.
Malatesta, L.C., Finnegan, N.J., Huppert, K.L., Carreño, E.I., 2021. The influence of rock uplift rate on the formation and preservation of individual marine terraces during multiple sea-level stands. Geology 50, 101–105.
Manspeizer, W., 1985. The Dead Sea Rift: impact of climate and tectonism on Pleistocene and Holocene sediments. In: Biddle, K.T., Christie-Black, N. (Eds.), Strike-Slip Deformation, Basin Formation and Sedimentation, 37. Society for Economic Paleontology and Mineralogy Special Publication, pp. 143–158.
Morin, E., Ryb, T., Gavrieli, I., Enzel, Y., 2019. Mean, trend and variance of Levant precipitation over the past 4500 years. Quat. Res. 91, 751–767.
Muhs, D.R., Kennedy, G.L., Rockwell, T.K., 1994. Uranium-series ages of marine terrace corals from the Pacific coast of North America and implications for last interglacial sea-level history. Quat. Res. 42, 72–87.
Muhs, D.R., Schweig, E.S., Simmons, K.R., 2020. Late Quaternary Sea-level history of Saipan, Commonwealth of the Northern Mariana Islands, USA: a test of tectonic uplift and glacial isostatic adjustment models. Geol. Soc. Am. Bull. 132, 863–883.
Mushkin, A., Katz, O., Crouvi, O., Alter, S.R., Shemesh, R., 2016. Sediment contribution from Israel's coastal cliffs into the Nile's littoral cell and its significance to cliff-retreat mitigation efforts. Eng. Geol. 215, 91–94.
Mushkin, A., Katz, O., Porat, N., 2019. Overestimation of short-term coastal cliff retreat rates in the eastern Mediterranean resolved with a sediment budget approach. Earth Surf. Process. Landf. 44, 179–190.
Naylor, L.A., Stephenson, W.J., Trenhaile, A.S., 2010. Rock coast geomorphology: recent advances and future research directions. Geomorphology 114, 3–11.
Nehorai, R., Lensky, I.M., Hochman, L., Gertman, I., Brenner, S., Muskin, A., Lensky, N.G., 2013. Satellite observations of turbidity in the Dead Sea. J. Geophys. Res. Oceans 118, 3146–3160.
Nicholls, R.J., Cazenave, A., 2010. Sea-level rise and its impact on coastal zones. Science 328, 1517–1520.
Wong, P.P., Losada, I.J., Gattuso, J.-P., Hinkel, J., Khattabi, A., McInnes, K.L., Saito, Y., Sallenger, A., 2014. Coastal systems and low-lying areas. In: Field, C.B., Barros, V.R., Dokken, D.J., Mach, K.J., Mastrandrea, M.D., Bilir, T.E., Chatterjee, M., Ebi, K.L., Estrada, Y.O., Genova, R.C., Girma, B., Kissel, E.S., Levy, A.N., MacCracken, S., Mastrandrea, P.R., White, L.L. (Eds.), Climate Change 2014: Impacts, Adaptation, and Vulnerability. Part A: Global and Sectoral Aspects. Contribution of Working Group II to the Fifth Assessment Report of the Intergovernmental Panel on Climate Change. Cambridge University Press, Cambridge, United Kingdom and New York, NY, USA, pp. 361–409.
Oviatt, C.G., Madsen, D.B., Miller, D.M., Thompson, R.S., McGeehin, J.P., 2015. Early Holocene Great Salt Lake, USA. Quat. Res. 84, 57–68.
Pedoja, K., Husson, L., Johnson, M.E., Melnick, D., Witt, C., Pochat, S., Nexer, M., Delcaillau, B., Pinegina, T., Poprawski, Y., Authemayou, C., Elliot, M., Regard, V., Garestier, F., 2014. Coastal staircase sequences reflecting sea-level oscillations and tectonic uplift during the Quaternary and Neogene. Earth Sci. Rev. 132, 13–38.
Roland, C.J., Zoet, L.K., Rawling III, J.E., Cardiff, M., 2021. Seasonality in cold coast bluff erosion processes. Geomorphology 374. https://doi.org/10.1016/j.geomorph.2020.107520.
Schuster, M., Nutz, A., 2018. Lacustrine wave-dominated clastic shorelines: modern to ancient littoral landforms and deposits from the Lake Turkana Basin (East African Rift System, Kenya). J. Paleolimnol. 59, 221–243.
Sirota, I., Arnon, A., Lensky, N., 2016. Seasonal variations of halite saturation in the Dead Sea. Water Resources Research 52 (9), 7151–7162.
Sneh, A., 1979. Late Pleistocene fan deltas along the Dead Sea rift. J. Sediment. Petrol. 49, 541–552.
Special Publication. In: Stewart, I.S., Vita-Finzi, C. (Eds.), 1998. Coastal Tectonics, 146. Geological Society, London, 378 p.
The ICDP Dead Sea deep drilling project. In: Stein, M., Goldstein, S.L. (Eds.), 2020. Quaternary Science Reviews, 249. https://doi.org/10.1016/j.quascirev.2020.106639 see specific papers in this volume.
Storz-Peretz, Y., Bowman, D., Laronne, J.B., Svoray, T., 2011. Rapid incision of a small, coarse and steep fan-delta in response to base-level fall: the case of Nahal Qedem, the Dead Sea Israel. Earth Surf. Process. Landf. 36, 467–480.
Street-Perrott, F.A., Harrison, S.P., 1985. Lake levels and climate reconstruction. In: Hecht, A.D. (Ed.), Paleoclimate Analysis and Modeling. John Willey & Sons, New York, pp. 291–331.
Striem, H.L., 1974. Mutual Independence of climatological seasons, as reflected by temperatures at Jerusalem 1861–1960. Isr. J. Earth Sci. 23, 55–62.
Sunamura, T., 1988. Beach morphologies and their change. In: Horikawa, K. (Ed.), Nearshore Dynamics and Coastal Processes. University of Tokyo Press, pp. 135–161.
Torfstein, A., Goldstein, S.L., Stein, M., Enzel, Y., 2013. Impacts of abrupt climate changes in the Levant from last glacial Dead Sea levels. Quat. Sci. Rev. 69, 1–7.
Torfstein, A., Enzel, Y., 2017. Dead Sea lake level changes and Levant palaeoclimate. In: In Enzel, Y., Bar-Yosef, O. (Eds.), Quaternary of the Levant: Environments, Climate Change, and Humans. Cambridge University Press, Cambridge, UK, pp. 115–126.
Vitousek, S., Barnard, P.L., Limber, P., 2017. Can beaches survive climate change? J. Geophys. Res. Earth Surf. 122, 1060–1067.
Waldmann, N., Neugebauer, I., Palchan, D., Hadzhiivanova, E., Taha, N., Brauer, A., Enzel, Y., 2017. Sedimentology of the lacustrine formations in the Dead Sea basin. In: Enzel, Y., Bar-Yosef, O. (Eds.), Quaternary of the Levant: Environments, Climate Change, and Humans. Cambridge University Press, Cambridge, UK, pp. 83–90.
Walkden, M.J.A., Hall, J.W., 2005. A predictive mesoscale model of the erosion and profile development of soft rock shores. Coast. Eng. 52, 535–563.
Young, A.P., Carilli, J.E., 2019. Global distribution of coastal cliffs. Earth Surf. Process. Landf. 44, 1309–1316.
Young, A.P., Guza, R.T., Matsumoto, H., Merrifield, M.A., O'Reilly, W.C., Swirad, Z.M., 2021. Three years of weekly observations of coastal cliff erosion by waves and rainfall. Geomorphology 375. https://doi.org/10.1016/j.geomorph.2020.107545.
Ziv, B., Dayan, U., Kushnir, Y., Roth, C., Enzel, Y., 2006. Regional and global atmospheric patterns governing rainfall in the southern Levant. Int. J. Climatol. 26, 55–73.